GEAR TECHNOLOGY

The Journal of Gear Manufacturing

JANUARY/FEBRUARY 1986

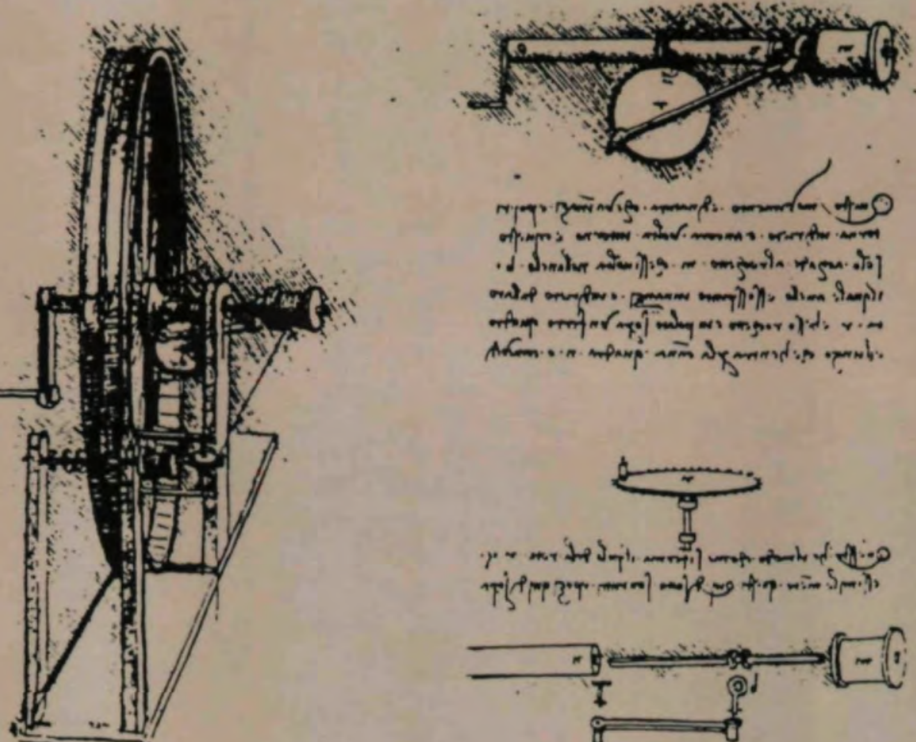

High Performance Grinding with CBN Wheels

Optimum Number of Teeth for Span Measurement

Effect of Shot Peening on Surface Fatigue Life

The Process of Gear Shaving

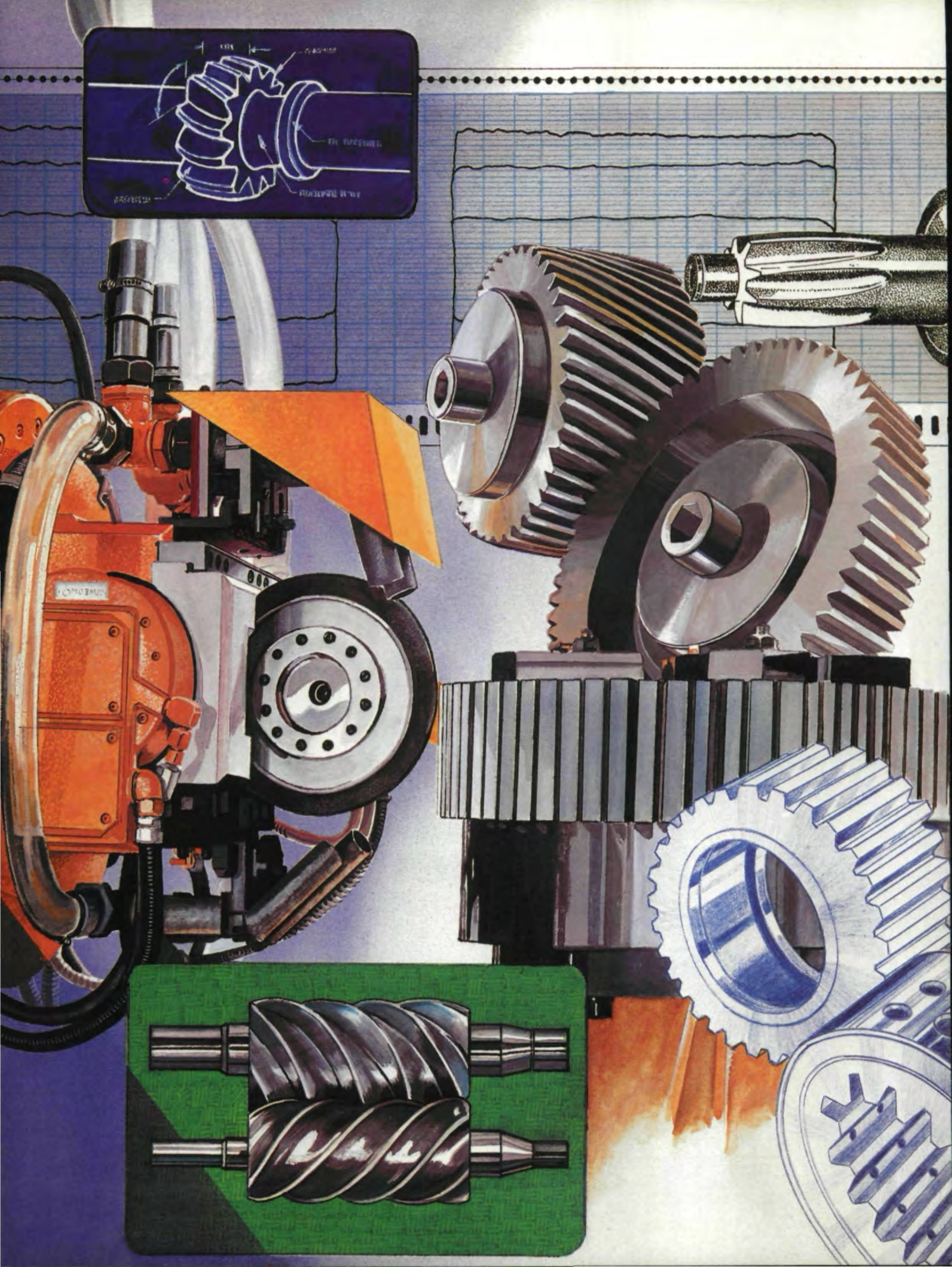

PUBLISHER & EDITOR-IN-CHIEF
Michael Goldstein

ASSOCIATE PUBLISHER & MANAGING EDITOR
Peg Short

BUSINESS MANAGER
Susan A. Johnson

EDITORIAL ASSISTANT
Patricia Flam

EDITORIAL SECRETARY
Pam Nolan

PUBLISHING CONSULTANT
Ray Freedman

ART CONSULTANT
Marsha Feder

TYPOGRAPHY:
Kenric Graphics, Inc.
Elk Grove Village, IL

PRINTING:
TCR Graphics
Streamwood, IL

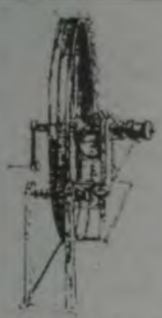

The Advanced Technology
of
Leonardo Da Vinci
1452-1519

COVER

Many of Leonardo's designs were to increase profitability. He tried to transform ancestral operations of his day and bring them into the industrial phase. One of the fields he applied his talents to was the textile craft. As a young man, he had learned this craft in Florence. Later he sketched many designs for improvement in this field.

The cover sketch is a design to ensure the even winding of thread onto a bobbin. The top sketch is an assembly view, and the bottom one is an exploded view. The crank was to turn the main shaft of the mechanism while the rod moved the bobbin axially in and out of the hollow shaft. This would enable the thread to be wound evenly on the bobbins face.

As was typical of many of Leonardo's designs, once the solution to a problem was solved, he abandoned it. He never realized the money that such improvements could have brought him.

GEAR TECHNOLOGY

The Journal of Gear Manufacturing

CONTENTS — PAGE NO.

FEATURES

DEPARTMENTS

January/February 1986 — Vol. 3, No. 1

GEAR TECHNOLOGY, The Journal of Gear Manufacturing (ISSN 0743-6858) is published bimonthly by Randall Publishing Co., Inc., 1425 Lunt Avenue, P. O. Box 1426, Elk Grove Village, IL 60007. GEAR TECHNOLOGY, The Journal of Gear Manufacturing is distributed free of charge to qualified individuals and firms in the gear manufacturing industry. Subscription rates for non-qualified individuals and firms are: $30.00 in the United States, $50.00 for foreign countries. Second-Class postage paid at Arlington Heights, IL and at additional mailing office.

Postmaster: Send address changes to GEAR TECHNOLOGY, The Journal of Gear Manufacturing, 1425 Lunt Avenue, P. O. Box 1426, Elk Grove Village, IL 60007

MANUSCRIPTS: We are requesting technical papers of every sort from manufacturers of gear making machinery and related equipment, universities, and engineers. Articles should be of an educational and training nature with general appeal to anyone having anything to do with the purchase of materials or machinery, or the design, manufacture, testing or processing of gears. Subjects sought are solutions to specific problems, explanations of new technology, techniques, designs, processes, and alternative manufacturing methods. These can range from the "How to . . ." of gear cutting **(BACK TO BASICS)** to the most advanced technology. All manuscripts submitted will be carefully considered. However, the Publisher assumes no responsibility for the safety or return of manuscripts. Manuscripts must be accompanied by a self-addressed, self-stamped envelope, and be sent to GEAR TECHNOLOGY, The Journal of Gear Manufacturing, P.O. Box 1426, Elk Grove, IL 60007, (312) 437-6604.

EDITORIAL

Photo by Jennifer Short

As I thought about what we might expect for 1986, the most important news affecting our industry is the tax revision bill just finished by the House Ways and Means Committee. Unfortunately, the final version of the committee's bill would eliminate or drastically reduce two of the most important incentives for the type of economic growth that pulled our nation out of the recession of the early 1980's — Investment Tax Credit (ITC) and Accelerated Depreciation.

The committee has refused to couple tax revision with progress on the nation's most pressing economic problem, its $200 billion deficit, and they failed to consider the overall economic impact of their proposals. It seems that they closed or opened loopholes depending on the clout of the people affected, not on the need to generate more jobs and make U.S. industries more competitive in world markets. ITC and Accelerated Depreciation will be removed just at the time American Industry is struggling to stabilize its position in world commerce.

The AGMA, the National Association of Manufacturers and hundreds of other business groups are trying to get across to the President and Congress that the removal of these incentives are both dangerous and unhealthy to our economic well being. If you ever felt inclined to write to your congressman, now is the time. Tell the President, your Representative and your Senator that the removal of the ITC and Accelerated Depreciation would be injurious to your industry and our country. They should vote against this bill as written and, if passed, it should be vetoed.

No matter what 1986 holds for us, we cannot let up on the intense effort which we are making to change our machines, our companies, our products, processes, and managements. We must continue to reinvest our profits, no matter how meager, to try and ensure our own future.

Michael Goldstein
Editor/Publisher

VIEWPOINT

Letters for this column should be addressed to Letters to the Editor, GEAR TECHNOLOGY, P.O. Box 1426, Elk Grove Village, IL 60007. Letters submitted to this column become the property of GEAR TECHNOLOGY. Names will be withheld upon request; however, no anonymous letters will be published.

Dear Editor

If I may, at this time, I would like to commend you and your staff for putting together a very excellent gear journal for the Industry. Every time I receive an issue of "GEAR TECHNOLOGY, The Journal of Gear Manufacturing", I always recall the meeting that we had in the spring of 1983 at which time you addressed your ideas in putting forth a technical journal to the industry.

As I travel around the country visiting with many of our customers, I am finding that not only are we, as an advertiser in the Journal, meeting our advertising needs, but you are also meeting those very high ideals that you put before us during that meeting. During these discussions with our customers, it has been indicated to me that you are addressing that area of technology that has previously been neglected by all other magazines in the area of gear manufacturing.

Martin C. Woodhouse
Sales Manager
Starcut Sales, Inc.

EDITORS NOTE: It is exciting for us that the readership of GEAR TECHNOLOGY continues to grow. In addition to our large domestic list, GEAR TECHNOLOGY is now being read in thirty foreign countries and requests for foreign subscriptions continue to come in daily. Thank you for the letters of encouragement that we continue to receive.

I am extremely glad to note that a journal exclusively meant for Gear Manufacture has at last been started. I have seen the June/July 1984 issue in a friend's place and I could not get the subsequent issues in India.

At present I am working as Chief Engineer in one of the largest gear

(continued on page 32)

The Leader In Gear Grinding Sets A New World Class Standard

The CNC Gear Grinder That Knows What to Do... When to Do It... and Does It!

Now, for the first time, a fully CNC 6-axis precision gear grinder is available to creep or conventional grind internal or external spur or helical gears up to 20-in. dia. with either vitrified or CBN wheels. Equipped with automatic stock dividing, the new Savoir Faire can be set-up for either single point, rotary disc or continuous form dressing. An electronically-controlled rotary table provides the required accuracy for lead generation and indexing.

Call or write Jim Ferrett, V.P. Marketing, for information and details on this significant development in gear grinding capability.

RED RING®

NATIONAL BROACH & MACHINE
A DIVISION OF LEAR SIEGLER, INC.

17500 TWENTY-THREE MILE ROAD • MT. CLEMENS, MICHIGAN 48044 USA • TELEPHONE 313/263-0100

CIRCLE A-2 ON READER REPLY CARD

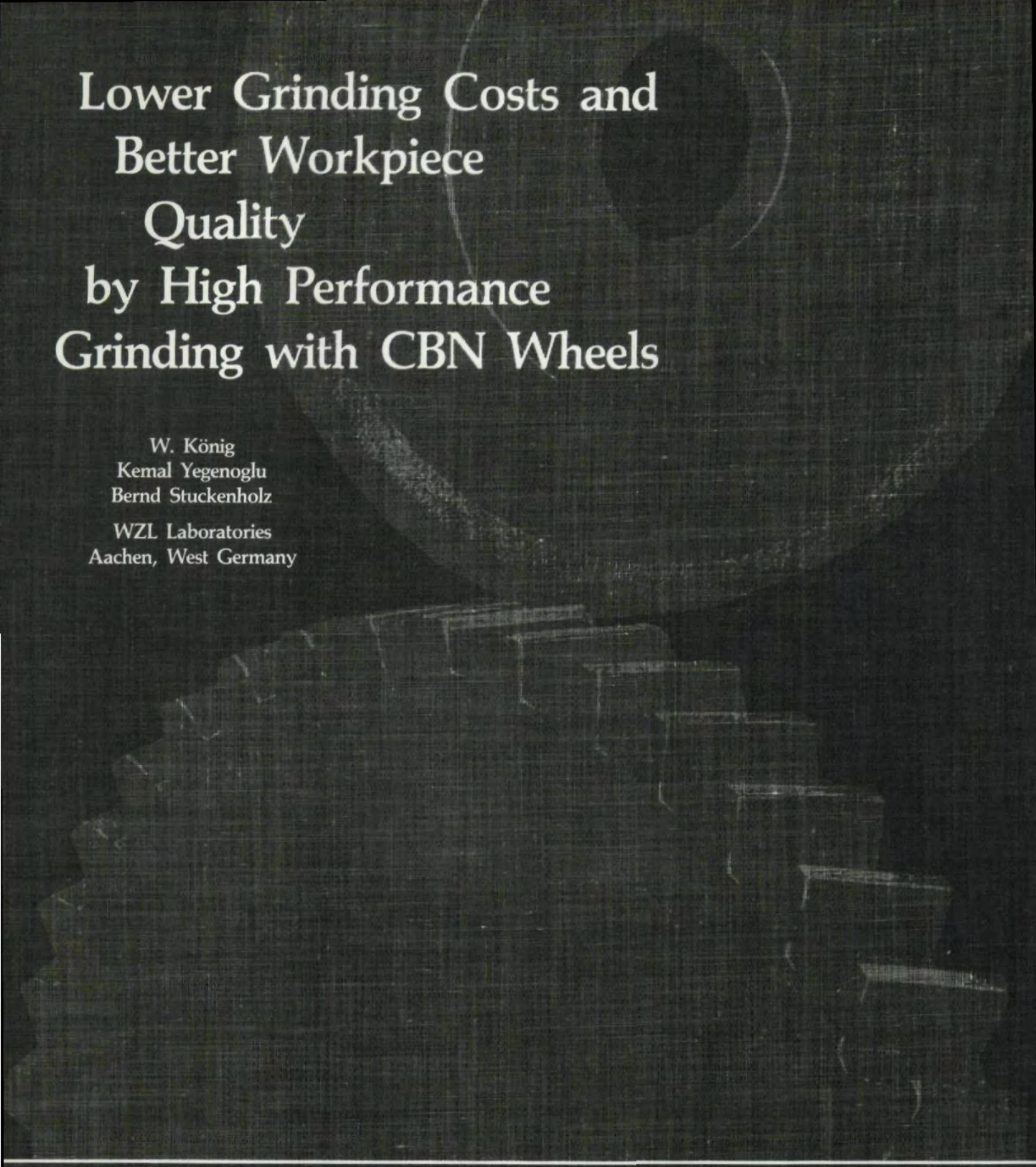

Lower Grinding Costs and Better Workpiece Quality by High Performance Grinding with CBN Wheels

W. König
Kemal Yegenoglu
Bernd Stuckenholz

WZL Laboratories
Aachen, West Germany

Introduction

A considerable improvement in the performance of the machining of hard to grind materials can be achieved by means of CBN wheels. CBN wheels feature resistance to wear and to heat development, and thus enable considerable reductions in production time without loss of quality.

However, the advantages offered by the abrasive CBN have to be weighed against disadvantages such as high wheel costs and technological and machine problems. Thus, considerable difficulties may be involved in:

- the correct grinding preparations for the CBN wheel with respect to the trueing and sharpening, and the selection of optimum machine parameters;
- the optimum selection of wheel specifications (grit size, concentration, bond type, bond hardness) for various applications, especially for high material removal rates and cutting speeds; and
- the inadequate capabilities of existing grinding machines with respect to cutting speeds and feed rates, drive power and rigidity.

Definition of terms:
Trueing: generating the macrogeometrical wheel shape within the required tolerances
Sharpening: generating a microgeometrical surface capable of grinding
Dressing: trueing and dressing taken together

This article is concerned with the complex problems outlined above. The optimization of the trueing and sharpening processes is vital for adaptation of the grinding wheel topography to the high requirements of the grindig process. A report is, therefore, given of trueing and sharpening systems that permit the generation of the required grinding wheel topography, assuming that the proper setting parameters are selected.

Additionally, an outline is given of the significance of the grinding wheel specification for the economic design of the process, and a survey is made of the influence of the machine parameters on the grinding result.

The article is concluded with an economic comparison between high-speed grinding with CBN and corumdum grinding.

Test Set-up and Test Parameters

The grinding process used in this test was drill flute grinding (Fig. 1). The drill flutes were ground in the creep-feed technique in a single pass.

The most important data for the test machine and constant test conditions are summarized in Table 1.

The workpiece material was hardened high-speed steel M2

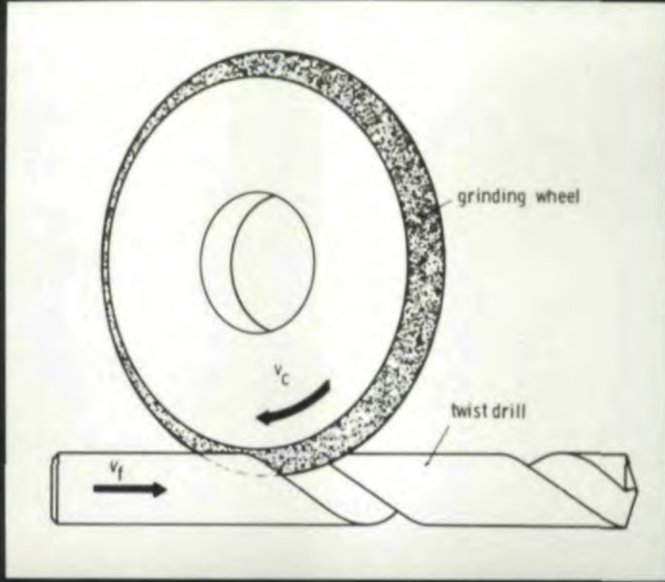

Fig. 1 – Process configuration for drill flute grinding

Drill flute grinding machine	
Type:	Gühring NS 335
Cutting speed:	v_c = 6500-23500 fpm (33-120 m/s)
Wheel diameter:	d_s = 16 in (400 mm)
Max. drive power:	P_{smax} = 80 hp (60 kW)
Feed rate:	v_f = 0-108 in/min (0-2750 mm/min)
Constant grinding parameters	
Material:	M2 (S 6-5-2) 64 HRC
Cutting speed:	v_c = 23500 fpm (120 m/s)
Feed rate:	v_f = 39;78 in/min (1;2 m/min)
Infeed:	a = 0,16 in (4,1 mm)
Material rem. rate:	Q'_w = 6,3 ;12,6 in^3/in · min (63;136 mm^3/mm · s)
Flute length:	l_n = 3,7 in (93,5 mm)
Workpiece diameter:	d_w = 0,4 in (10 mm)
Grinding width:	b_s = 0,2 in (5 mm)
Coolant:	Oil
Coolant supply:	Pressure chamber
Coolant flow:	Q_s = 32 gallon/min (120 l/min)

Table 1: Machine Data and Constant Grinding Parameters

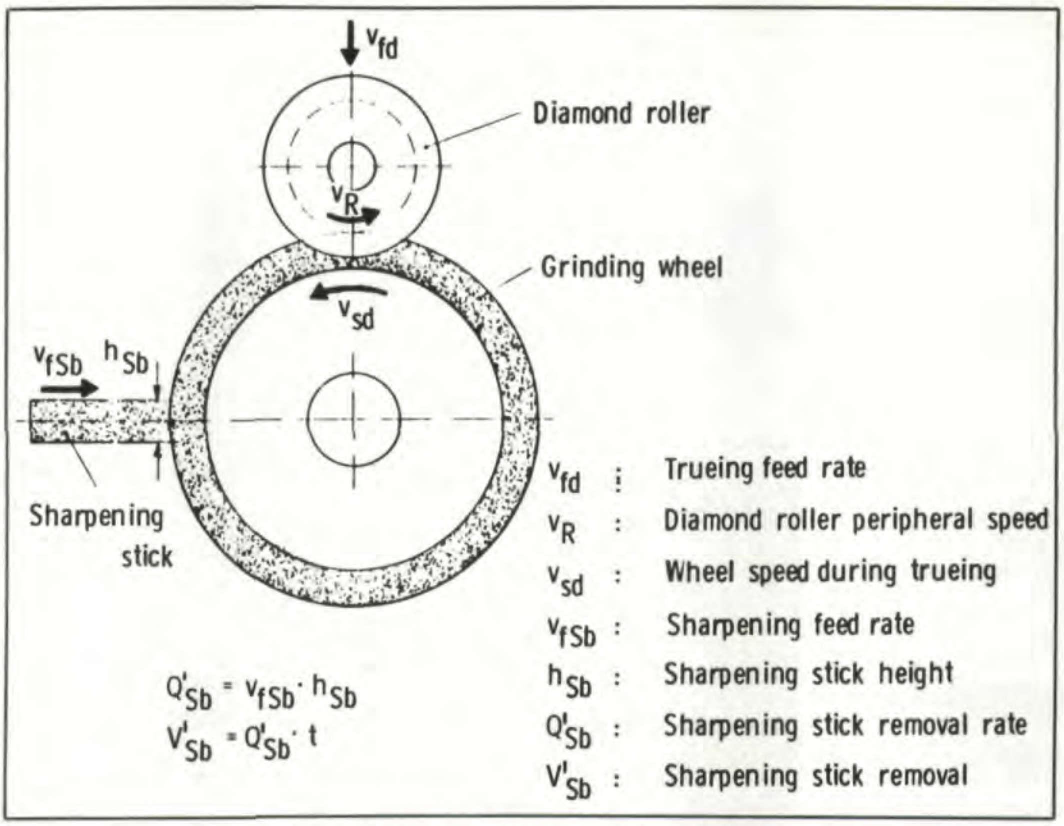

Fig. 2—Configuration of trueing and sharpening tools

(65 Rockwell cone). The coolant supply was effected with the aid of a pressure chamber system. The resinoid bond CBN wheels were trued with a diamond profile roller, and then sharpened with a corundum stick in a plunge technique. The schematic arrangement of a grinding wheel, trueing roller and sharpening stick is shown in Fig. 2.

Grinding Preparation of CBN Wheels

The grinding preparation of a multiple layer CBN wheel, divided into the trueing and sharpening operations, is one of the main problems of CBN grinding technology.

CBN wheels in resinoid bonds, permitting high grinding speeds ($v_c \geqslant 17,650$ fpm), can be trued quickly and accurately without dismounting them from the grinding spindle, by the means of a diamond trueing roller, or profile roller.[2,3]

After trueing with a diamond roller, the surface of the CBN grinding wheel has no more grit protrusion (Fig. 3, top). The CBN grits and their bonds are cleanly cut. Additionally, there are recesses, or holes, in the bond—this is where the grits have been partly or completely removed from their bonds.[1,4]

The grinding wheel is not capable of cutting when it is in this condition. The bond material between the CBN grits must be set back by a certain amount in order for the coolant to be transported to the contact zone, and also to provide enough space for chip removal from the contact zone. The process of setting back the bond is known as sharpening. This is done by feeding a corundum sharpening stick into the grinding wheel surface at a constant feed rate. Variations in the sharpening parameters cause a considerable variation in the wheel topography, so that the optimization of the sharpening process is extremely important.

The middle row of the photos shows the wheel surface that is generated with comparatively small sharpening stick removal rates and removal volumes. The cutting edges of the grits protrude from the bond, and they are supported at the

AUTHORS:

DR. WILFRIED KONIG *is the Director of the Fraunhofer-Institute for Production Engineering, Aachen, West Germany. He received his engineering degree from the Technical University Aachen and subsequently earned the degree of Dr. Ing.. In 1966 he was a lecturer for "Material Cutting Machining," and he has served as the Chairman of Technology of Production Processes and Director of the Machine Tool and Production Engineering Laboratory. Additionally, Dr. Konig has held various functions on University Committees, scientific and technical associations.*

MR. KEMAL YEGENOGLU *has been Assistant at the Machine Tool and Production Engineering Laboratory (WZL) of the Technical University of Aachen since 1980. He received his degree in Mechanical Engineering from the Technical University, Aachen in 1980.*

MR. BERND STUCKENHOL *studied Mechanical Engineering concentrating especially on Manufacturing Engineering at the Technical University of Aachen. He earned his degree in 1982 and since that time has also served as Assistant in the Machine Tool and Production Engineering Laboratory (WZL).*

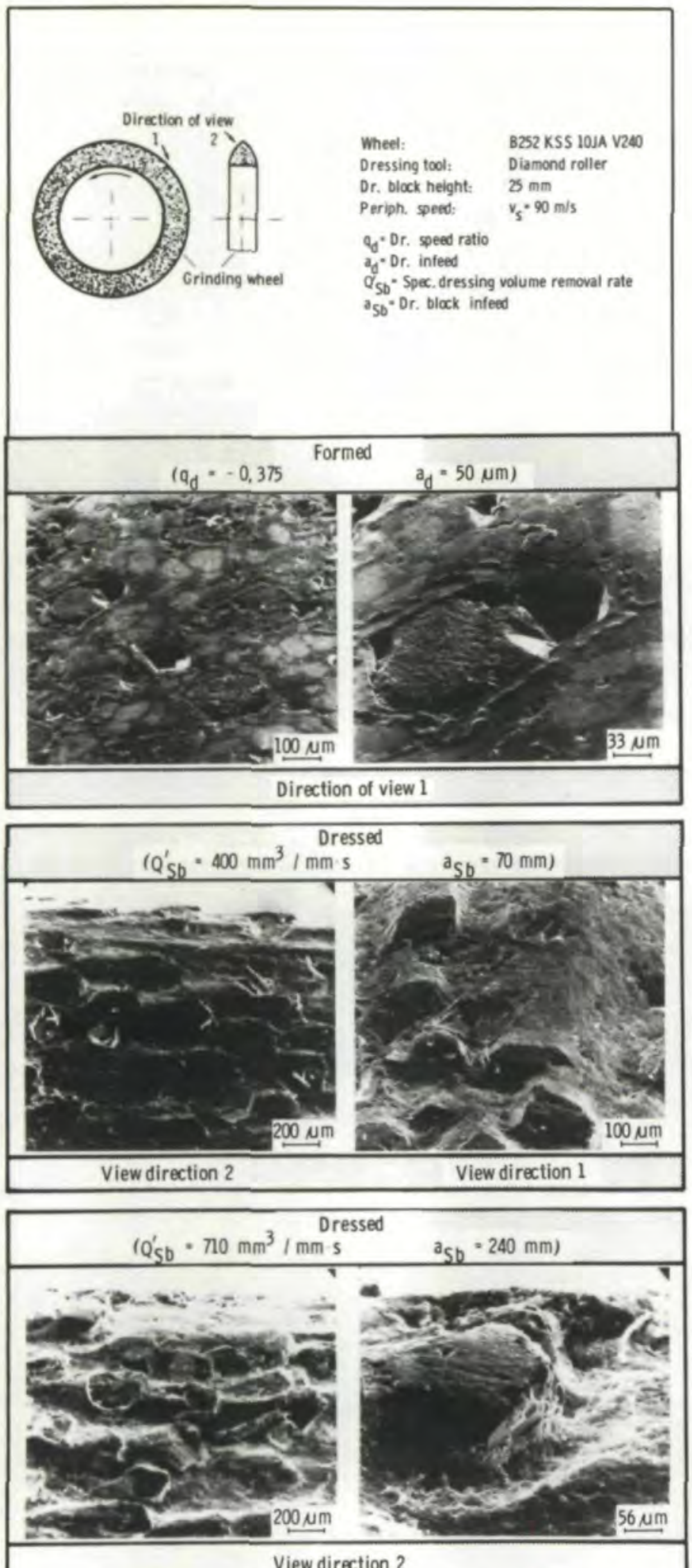

Fig. 3 – The wheel cannot grind until it has been sharpened

rear by a bond backing that helps to retain them during the grinding process.

If the sharpening stick is fed in at a very high feed rate, there is a topography change due to the considerable increase in grit protrusion. This decreases the retention of the CBN grits in the bond with considerable grit breakout due to the forces exerted. If the sharpening process is too long, i.e. too

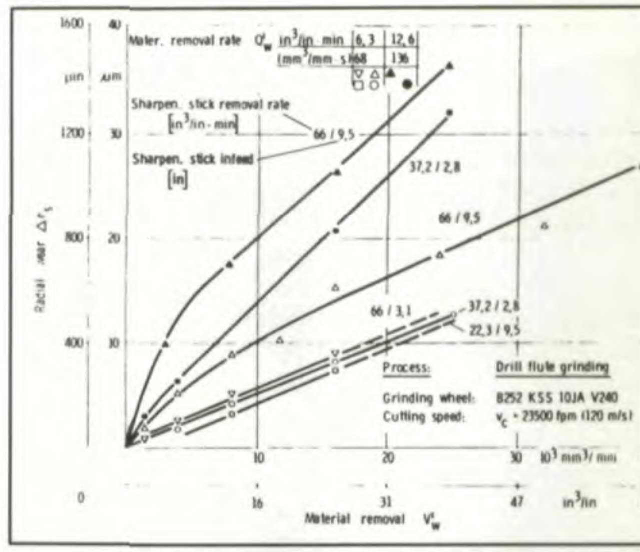

Fig. 4 – Optimization of sharpening process minimizes wear

much sharpening stick volume is removed, wheel topography is likewise changed due to bond erosion.

The bottom row of the pictures shows part of the surface of a grinding wheel which has been sharpened with approximately double the feed rate, and three times the volume of corundum sharpening stick. Bond removal is particularly great in the immediate vicinity of the grit, as the corundum particles pile up in front of the CBN grit and flow around its sides.

The sharpening stick feed, or sharpening stick removal rate, and the sharpening stick removal must thus be set in such a way as to generate an optimum grinding wheel topography for the subsequent grinding process, that is dependent on the grinding wheel specification and machine parameters.

The effect of sharpening behaviour on the grinding process will now be illustrated by considering wheel wear, as shown in Fig. 4. If the sharpening conditions are too hard, this has a negative effect on wear behaviour, as can be seen from the lower family of curves for $Q'_w = 6.3$ in^3/in.min. The bond is set back a long way and the CBN grits are loosened by excessively long sharpening ($Q'_{Sb} = 66$ in^3/in.min, $a_{Sb} = 9.5$ in), which causes a considerable increase in the wheel wear. An optimization of the sharpening conditions provides considerable reduction in initial radial wear.

The sharpening stick removal rate at which the specified wheel topography, characterized by the peak-to-mean-line height R_{ps} of the wheel, is generated, can at present be calculated by the application of a mathematical model. Further parameters which are included in the model are the wheel specification and the wheel peripheral speed during sharpening:

$$Q'_{Sb} = 0.95\, q_m^{-1} \sqrt{c_k \left(1 - \frac{R_{ps}}{w_m\, q_m\, \epsilon_{crit}}\right) R_{ps}^{5/2}\, v_c} \quad (1)$$

Where:

qm : longitudinal stretch coefficient of the CBN grits ($q_m = 1.41$

c_k : no. of grits per volume unit of grinding layer

R_{ps} : peak-to-mean-line height of grinding wheel

w_m : mean mesh width

ϵ_{crit} : critical grit protrusion related to grit diameter

v_c : cutting speed during sharpening

The number of grits $c_k$and the mean mesh width $w_m$are dependent on the grinding wheel specification, and can be taken from the corresponding tables.[1]

The critical grit protrusion ϵ_{crit} is an expression for the amount that a grit can protrude over the bond level without breaking out under the forces exerted during sharpening. Tests gave a value of $\epsilon_{crit} = 44$-46% for resinoid bond wheels. The peak-to-mean-line height of the wheel R_{ps} describes the chip space generated by the bond removal. Due to the integral character of this expression, its reaction to individual holes in the bond caused by grit breakout is relatively insensitive. An R_{ps} value of 25-30% of grit diameter has led

Single flank testing goes digital.

FIND OUT WHAT THE NOISE IS ALL ABOUT.

When it comes to pinpointing the causes of gear vibration and noise, it's no secret that single flank measurement gives you the kind of comprehensive data you simply can't get with other forms of measurement. Reliable information about *transmission error* is what you need to predict noise potential of a gear set in operation, as well as to reduce process errors and the costly scrap and rework that go with it.

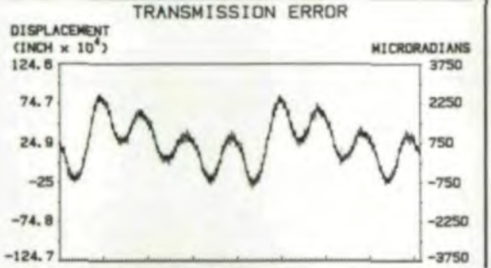

But the analog (graphic) results of single flank testers can be time consuming to analyze—even for an experienced operator. So single flank testing hasn't always been practical for production environments.

Until now.

Gleason gives single flank testing "brains."

With Gleason's 579 G-AGE™ Automatic Data Analysis System, ADAS (compatible with any G-AGE Single Flank Tester), test results are generated digitally and graphically to greatly reduce data interpretation time. Featuring the most sophisticated single flank software available today—a Gleason exclusive—this intelligent system rapidly and accurately:

1. Quantifies single tooth-to-tooth composite error, combined pitch variation, combined accumulated pitch variation, single flank composite error and other gear tooth variations.
2. Reveals the noise potential of gear sets.

And with our system's frequency spectrum analysis, the harmonics and side bands of tooth mesh frequency can be observed to let you establish acceptable peak amplitudes for various harmonics. That means you can be sure of a gear's noise potential before it's assembled.

GLEASON AUTOMATED GEAR EVALUATION

	TOLERANCE	MEAS. ERROR	PERCENT OF TOL.
TOT. TRANS. ERROR	+.0060	+.00520	+++++
MAX T-T TRANS. ERROR	+.0007	+.00050	++++
AVG T-T TRANS. ERROR	+.0002	+.00020	REJECT
# OF BURRS OVER TOL	+3.0000	+0.00000	
MAX EFFECTIVE PROF VAR	+.0003	+.00010	++++
AVG EFFECTIVE PROF VAR	+.0002	+.00010	+++
COMB. ACC. PITCH VAR	+.0050	+.00500	REJECT
COMB. MAX PITCH VAR	+.0007	+.00050	++++
COMB. MAX SPACING VAR	+.0015	+.00030	++

(RESULTS IN IN)

Let our brain help your brains be more productive. Call Gleason's Sales Department today and arrange an in-depth, no-obligation consultation about our new 579 G-AGE ADAS.

Call this number today:
(716) 473-1000

Gleason

The Gleason Works, 1000 University Avenue, Rochester, N.Y. 14692

CIRCLE A-10 ON READER REPLY CARD

to satisfactory results in the investigations made so far. Research work is at present being carried out for a precise description of the peak-to-mean-line height R_{ps} adapted to the process parameters (cutting speed v_c, specific material removal rate Q'_w, workpiece material characteristics).

Fig. 5 shows the functional relationships with the aid of a nomogram. This form of presentation makes it possible to determine the specific sharpening stick removal rate for any values of the above variables, starting from the wheel specification, and proceeding via the critical grit protrusion ϵ_{crit}, peak-to-mean-line height R_{ps} and cutting speed v_c.

The specification of the sharpening stick removal rate must be followed by the determination of the sharpening stick removal. The characteristic of sharpening force or grinding power can be used for this purpose. During the sharpening process, these two characteristics drop from high initial values to steady state final levels. In this steady state phase, the bond removal has practically come to a standstill. If the sharpening process is stopped here, this results in the favorable linear wear behaviour of the grinding wheel, which is possible with this sharpening stick removal volume. Further infeed of the sharpening stick beyond this time gives no major bond removal, but in any case it loosens the CBN grits and, thus, causes excessive initial wear.

A further measure for the optimization of the sharpening process would be simultaneous trueing and sharpening.[5] This modified procedure, i.e. the infeed of a sharpening block during the trueing process itself, not only gives a reduction in trueing time, but also permits the achievement of considerably longer dressing roller life as shown in Fig. 6.

Here the sharpening stick has the task of setting back the bond continuously, so that the dressing roller simply removes the protruding CBN grits, and does not come into contact with the bond. Without the sharpening stick infeed, the diamond crystals of the dressing roller would not only cut the CBN grits, but also the tough bond mass, resulting in high friction, high temperatures and consequently high wear of the diamond grits. A further advantage of simultaneous trueing and sharpening is that the wheel has a slightly rough surface after a profiling process of this kind. This reduces the time required for the subsequent sharpening process.

Influence of Grinding Wheel Specification

In addition to optimization of the trueing and sharpening parameters, careful wheel selection has also the purpose of achieving the best possible combination of workpiece quality, machining time and tool life. A comparison is therefore made below of the grinding behaviour of resinoid bond CBN

$$Q'_{Sb} = 0{,}95\, q_m^{-1} \sqrt{c_k \left(1 - \frac{R_p}{w_m\, q_m\, \varepsilon_{krit.}}\right)}\, R_p^{2,5}\, v_c$$

Longit. stretch coeff. $q_m = 1.41$ (CBN)

Grit size US-Mesh	Grit size FEPA	Mesh w_m [µm]	Grit concentration $K \cdot 10^3$: 60	120	180	240	300
240	64	58	416	833	1250	1666	2082
180	91	83	142	284	426	569	711
150	107	98	86	173	259	345	432
120	126	117	51	101	152	203	254
100	151	137	32	63	95	126	158
80	181	165	18	36	54	72	90
60	251	231	6,6	13	20	26	33
			Grit density c_k [mm^{-3}]				

$c_k = \frac{6}{\pi} \frac{K}{q_m w_m^3}$

$q_m = 1,41$

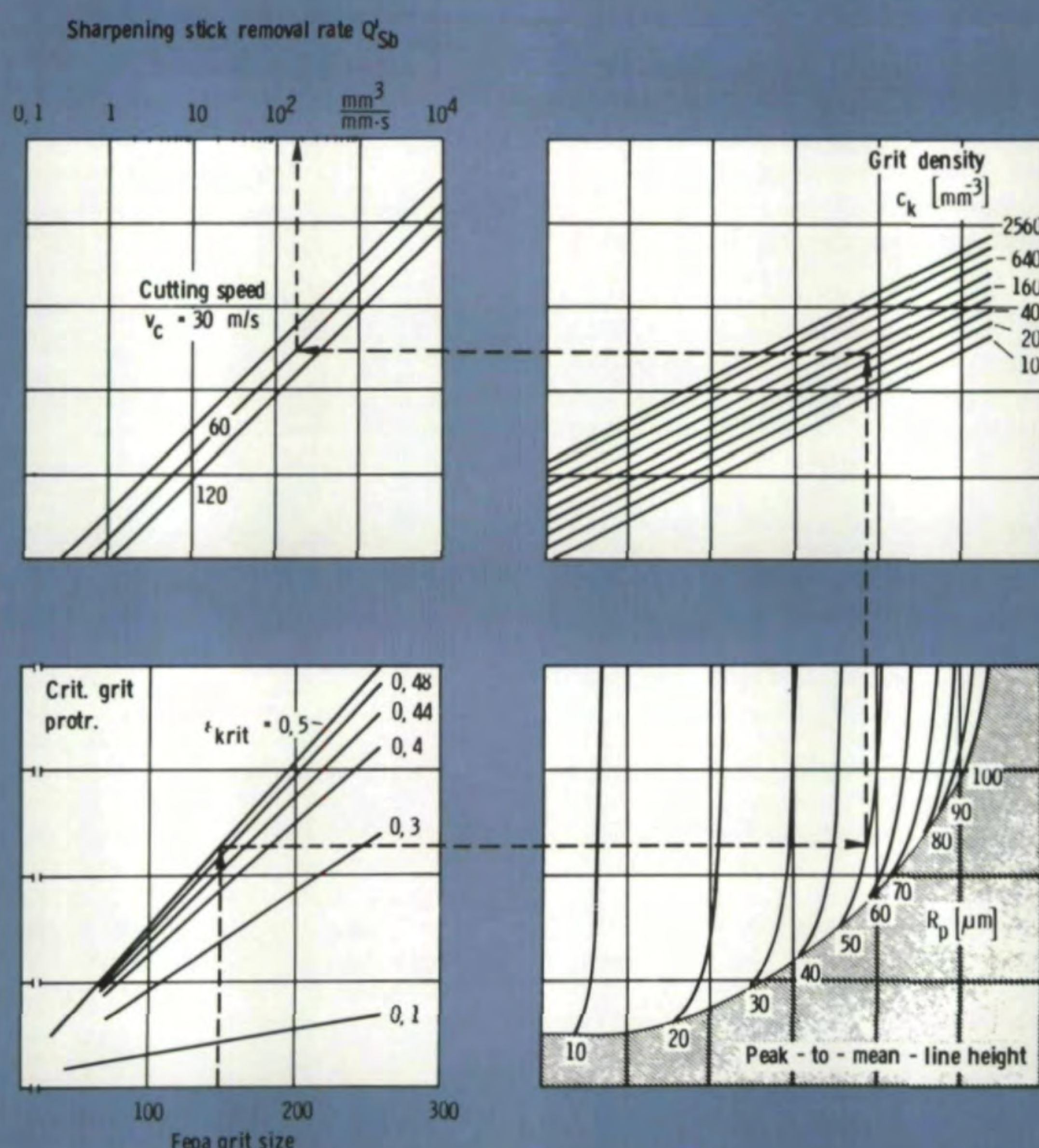

Fig. 5 – Nomogram for determination of sharpening material removal rate

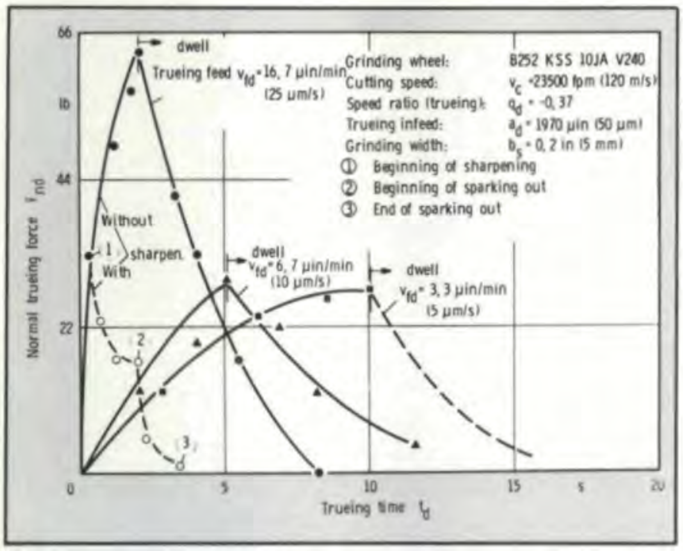

Fig. 6 – Simultaneous trueing and sharpening minimizes dressing time and increases trueing tool life

wheels of different grit size, concentration and bond hardness.[6] The advantages and disadvantages of electroplated wheels in high-speed grinding are subsequently discussed.[7]

Resinoid Bond Wheels

One of the causes of progressive wear of a grinding wheel is a change in grit geometry during the machining process. Thermal, chemical or mechanical stresses result in a dulling of the cutting edges that are engaged in the cutting process; this is designated as grit wear Δr_k.

However, grit geometry changes are not the only reason – wheel wear is also caused by breakout of complete grits. The factors determining grit breakout are the combination of the stress attacking the individual grit and the capability of the bond material to retain the grit under this stress. Fig. 7 shows the principle of the chain of effects leading to grit breakout, neglecting the influences from machine parameters and grinding wheel specifications.

Dulling of the grits causes greater friction with the workpiece material, increasing the individual grit force F_k. Considering the material characteristics of the bond as a constant for the moment, the depth of bond embedding is decisive for whether or not the grit breaks out under the load. The embedding depth and, thus, the grit protrusion is determined by the cutting products which set back the bond in the area of the grit so far that there is sufficient chip space available. In order to maintain this space, the embedment depth is constantly reduced with increasing grit wear Δr_k, so that the force $F_{k\,max}$ required for grit breakout also constantly decreases. The opposite tendency of the individual grit force F_k and the grit breakout force $F_{k\,max}$ automatically leads to grit breakout when the equilibrium of force is attained.

Considering the effect of changes in machine parameters and grinding wheel specifications, it is possible to differentiate between those that affect individual grit force and those that affect grit breakout force. Grit loading is determined by

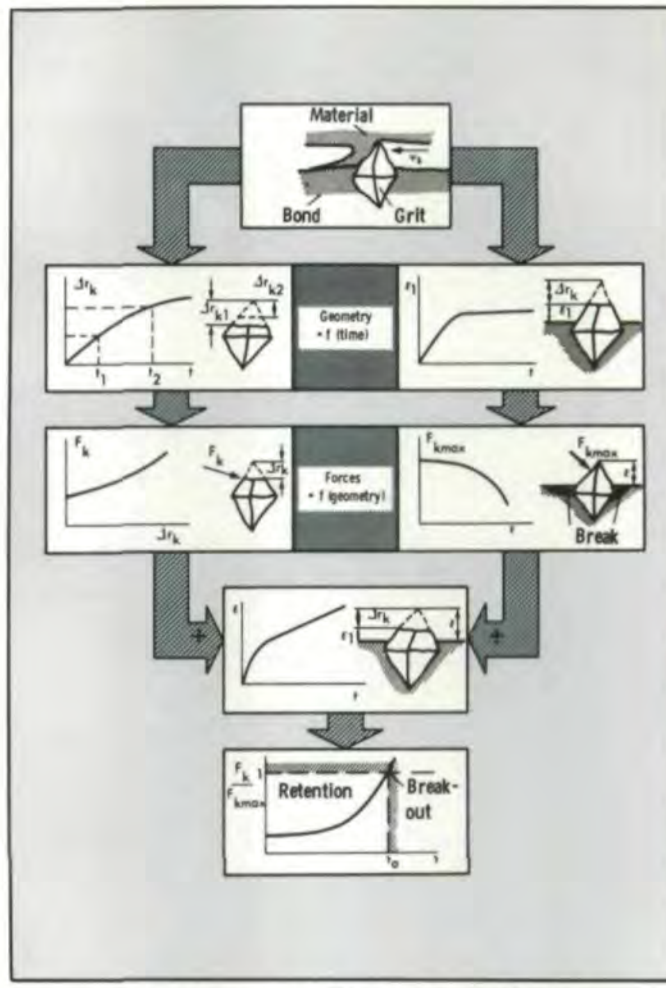

Fig. 7 – Wear on grit and bond lead to grit breakout

the number of cutting edges which, depending on the wheel specifications and the machine parameters, are involved in the cutting process and to which the cutting forces are distributed. Thus, a higher grit load might either be caused by an increase in material removal rate or by a decrease in cutting edge density c_k (number of grits per volume unit, Fig. 8), as results from larger grit size or lower grit concentration.

The level of grit breakout force and the embedment depth at which grit breakout occurs depends decisively on the bond material and on the grit use. Larger grits are better anchored in the bond and thus permit higher cutting edge load. Model investigations on ideal octahedral grits showed a load capability rising with the square of the grit diameter for constant relative embedment depth.

With all the grinding wheels examined, a doubling of the material removal rate resulted in a considerable decrease in the grinding ratio, which was to be expected in view of the higher grit load and the greater chip room requirement.

A comparison of grit sizes shows that the smaller grit B 151 is considerably superior to B 252 for both the bond types and removal rates as shown in Fig. 9.

Assuming that the kinematic cutting edge number $N_{k\,in}$, i.e. the number of grits involved in the cutting process, changes in the same proportions as grit density, it is only 21%

Grit size US-Mesh	Grit size FEPA	Mesh w_m [µm]	Grit concentration, K · 10^3: 60	120	180	240	300
240	64	58	416	833	1250	1666	[illegible]
180	91	83	142	284	426	569	711
150	107	98	86	173	259	345	432
120	126	117	51	101	152	203	254
100	151	137	32	63	95	126	158
80	181	165	18	36	54	72	90
60	251	231	6,6	13	20	26	30

Grit density c_k [mm^{-3}]

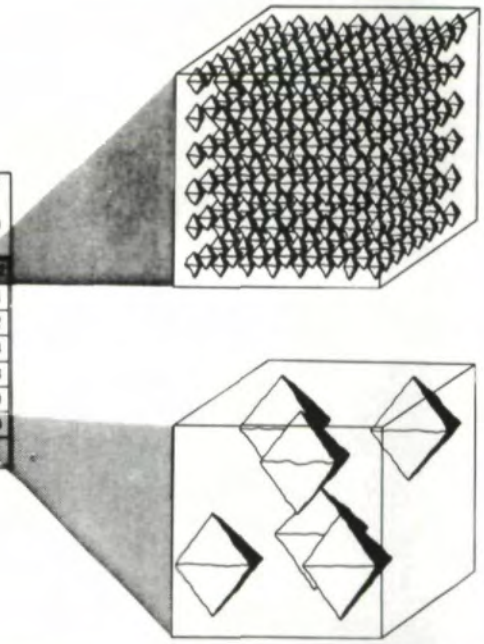

Fig. 8—Grit density increases progessively with decreasing grit size

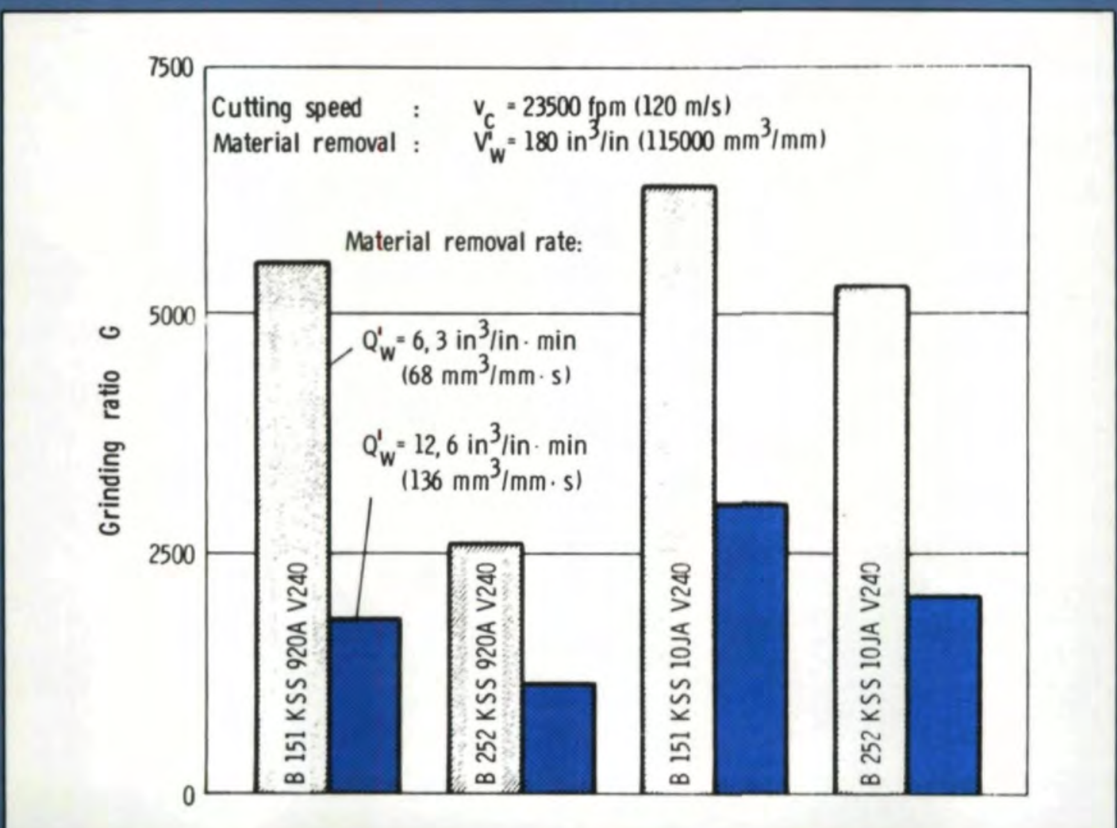

Fig. 9—Lower loading of smaller grit sizes increases life

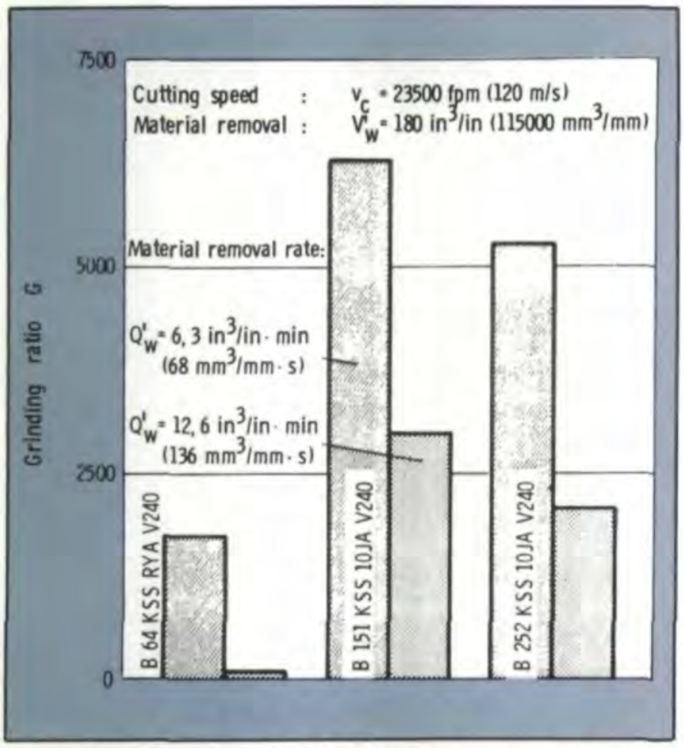

Fig. 10 – Bond wear and grit load determine optimum grit size

for B 252 in relation to B 151. This means that the individual grit load is 5 times as high for B 252. This is opposed by an increase of grit breakout force of only 2.8 times. The larger grit is, thus, subject to relatively higher load, and this results in earlier grit breakout, i.e. faster wear. However, these considerations are only applicable if bond wear caused by the chips plays only a subsidiary role. If the grit size is reduced, e.g. to B 64, this brings no further improvement in the G-ratio as shown in Fig. 10.

Although the smaller grit (B 64) has a more wear resistant bond (hardness R), the G-ratio is only a fraction in comparison with larger grits, especially for a material removal rate $Q'_w = 12.6$ in^3/in.min.

Although chip thicknesses and grit loads continue to decrease in accordance with the above considerations, the long chip lengths typical of the creep-feed grinding process are still present. As the possible grit protrusion is only small, the abrasive attack of the chips on the bond is obviously too great. Therefore, it requires little wear for the grits to break out, since bond level constantly drops below the critical embedment level. The material removal rate is well above the limits for this wheel.

The wear effect of "grit load" and "bond removal" are opposed when plotted against grit size. This means there is a maximum G-ratio, which is in the range of grit size B 151 for the grinding parameters considered here. For milder grinding parameters, i.e. lower material removal rates, this optimum will shift towards smaller grit sizes and vice versa.

A comparison of the bonds shows that in the high-speed grinding process considered, the 10J bond is clearly superior to the 920 bond. In particular for high material removal rate and coarse grit, i.e. with the parameters which make the highest demands on bond strength, the G-ratio is about twice as high for the 10J bond as it is for the 920 bond.

In addition to grit size and bond hardness, the grit concentration, also, has a considerable influence on the working result.

Fig. 11 shows the results of investigations carried out with two wheels of different concentration. The grit concentration was 18% and 30% by volume respectively, and the bond hardness was further increased by selection of the bond type RY.

If there is a lower grit concentration in the grinding layer (V 180), there are fewer cutting edges involved in the cutting process, which means that the load on the individual cutting edges is higher. This negative influence on the individual grit forces can, however, be compensated by greater bond hardness, i.e. by increase of the force necessary for grit breakout. This means that with very hard bond and low grit concentration (B 252 KSS RY A V 180) the G-ratio is already the same as for grinding wheel with soft bond and higher grit content (B 252 KSS 10J A V 240).

An increase in concentration to 30% by volume increases the wheel price, but it also permits an increase in G-ratio by more than 100% as compared with the wheel having a concentration of 18% by volume.

Test results have shown that the selection of a harder bond and a suitable grit size make it possible to reduce wheel wear considerably. An increase in grit concentration likewise has a positive effect on wheel wear. Thus, it might be expected that a combination of the hard bond (RY) and the high concentration (V 300) would achieve the highest G-ratio.

Electroplated Bond Wheels

Electroplated bond CBN wheels have only a single layer of CBN as an abrasive, i.e. the layer thickness corresponds approximately to the mean grit size used.

Fig. 11 – High concentration and hard bond increase life

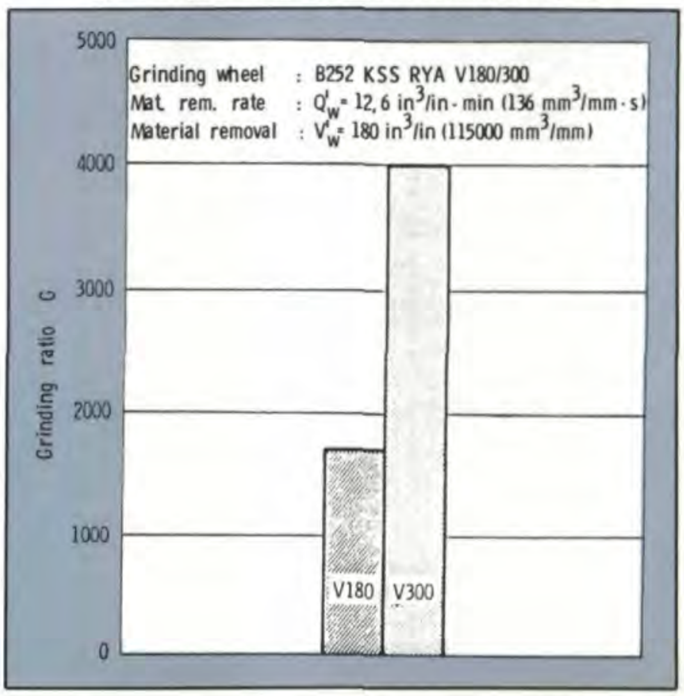

The production of these wheels is based on deposition of nickel or nickel alloy on the appropriate bases, and simultaneous inclusion of CBN grits in the bond. Single layered wheels of this kind permit cost effective production of complicated shapes, since profiling is effected on the base and it is not necessary to manufacture sintering molds, which is very expensive for small quantities.

A further advantage of electroplated bond wheels is that they do not have to be dressed. There is no necessity for the complicated trueing and sharpening devices or for the required technologies, which are often difficult to master unless a very high profile quality is not needed.

The position of the CBN grits in the bond structure has a favorable effect with respect to thermal boundary layer influence. The individual grit is not a part of a multiple grinding layer, where some of the grits cutting the workpiece material are dulled by dressing. Here the CBN grit protrudes undamaged from the bond. Electroplated bond CBN wheels are, therefore, always sharp and in new condition, and permit grinding without thermal problems at the usual material removal rates.

However, there are also disadvantages. Whereas with multiple layer wheels, minor radial runout can be eliminated by trueing, time consuming adjustment is required with electroplated bonds. Axial runout likewise has to be minimized during this adjustment in order to ensure satisfactory working of the wheel at high cutting speeds.

A serious disadvantage of this type of bond in high speed grinding is the fact that the grinding behavior of the wheel, and thus, the result of the grinding process does not remain constant. With a new wheel only the CBN grits that protrude the furthest from the bond level engage the workpiece. The sharpness of the cutting edges and their small number give small cutting forces and large roughness heights. As the engagement time progresses the sharp grits are gradually dulled, so that the lower lying grits come into engagement causing the number of grits increases. The cutting forces and the mateial removal rate increase, while the roughness height decreases. As the grinding wheel topography cannot be regenerated by a trueing process, electroplated bond wheels continue to provide uneven grinding results up to the end of their service life.

Four electroplated bond CBN wheels were used in the investigations into drill flute grinding, these had identical GSS bond, but differed in their grit type and grit size. Two wheels contained CBN grit of microcrystalline structure with friable characteristics, and thus greater self-sharpening capability (CBN B), while the other two contained a conventional, more monocrystalline CBN grit (CBN A). The grit sizes B 151 and B 252 were investigated for each grit type.

The grinding tests were continued until the end of the life of the respective wheels, which is annnounced by the smoothing of the wheel surface, and by the progressive increase in cutting forces and grinding power input. With the wheels using the conventional CBN A grit, the grinding layer was already loose after grinding a small number of flutes.

The influence of the number of flutes, i.e. the removal volume, on the cutting forces is shown in Fig. 12. For all wheels, the cutting forces increase with increasing removal volume, whereby, this increase is degressive with the coarse grit wheels and progessive with the fine grit wheels.

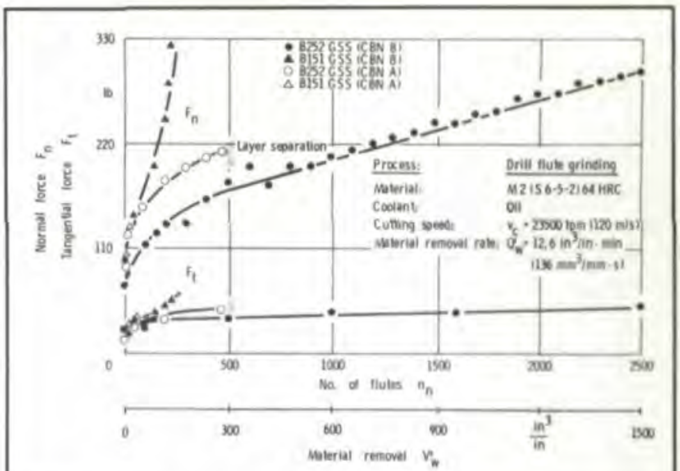

Fig. 12 – Electroplated wheels with small grit size generate higher cutting forces and have much shorter life

Due to smaller mean grit diameter, the CBN grits are obviously not retained firmly enough in the bond with the specification B 151, and break out when subjected to relatively small loads. In addition the bond is subjected to a greater load with the fine grit wheels, since the chip room is not large enough for the chips. There is a crushing process between chip, bond and grit. The simultaneous loading of bond and grit increases wear and the number of grit breakouts. The fast dulling of the grits increases the friction area, and the number of cutting edges increases rapidly. This causes progressive increase in forces as described above.

With the larger specification grit (B 252), grit abrasion and grit breakout are slower. The bond is subject to a smaller load due to the large chip spaces. The number of cutting edges increases more slowly, and the force characteristic shows only a degressive increase.

Fig. 12 also shows that the grit (CBN B) causes smaller forces than the conventional grit (CBN A). The tendency to friability and self-sharpening of grit type CBN B has a positive effect in this connection. Thus, grit type B 252 gives a force level that is 30-40% lower than grit type CBN A.

The electroplated bond CBN wheels examined give a high average roughness height, unlike corundum wheels or multiple layer CBN wheels. This is mainly because the CBN grits protrude from the electroplated bond. The resulting large chip thicknesses lead to a rough workpiece surface. The average roughness height R_z, which was measured in each case at the flute flanks, was about 160 micro inches at the beginning of the grinding process. However, due to the dulling of the sharp edges and to the sharp corners of the CBN grits, these high initial values decreased to 80 micro inches with the increasing number of flutes ground.

With the wheel in unworn condition, a low number of cutting edges combined with the high workpiece roughnesses and low cutting forces mean that no thermal problems should be expected in the grinding processs. All the wheels tested permitted grinding without damage at low removal volumes and low number of flutes ground ($n_n = 1 - 10$).

However, the longer the grinding process continues, the more the wheel becomes dull with consequent increase of cutting forces as described above. The frictional heat and contact zone temperature likewise rise, with consequent thermal boundary layer influence in the workpiece. (Fig. 13)

Thus after grinding of 500 flutes with the wheel B 252 (CBN B) there was already a clearly visible thermal damage zone which becomes wider from the flute center towards its back. Finally, after grinding of 2600 flutes the entire cross section is affected, so that the major cutting edge of the drill is likewise damaged.

If thermal damage is a limit criterion for workpiece quality, the tool life of the electroplated bond CBN wheel is relatively low for the thermally critical high speed grinding process considered. In addition, adaptation of the tool to the respective machining tasks is only possible by selection of grit size and type. With resinoid bonds this adaptation can be done much more precisely by additional optimization of the concentration, bond hardness and trueing and sharpening parameters.

Machine Concepts

The potential performance increases possible with high speed grinding can only be realized, if the machine design is suited to the extreme requirements of the process. First of all the positioning drives must be designed to handle the speed and torque necessary for high material removal rates and reaction forces, whereby, uniformity of the movements is especially important for a stable process.

The large material removal rates involved necessitate grinding spindles capable of handling forces up to about 2200 lb per inch grinding width in the speed range 6000 to 9000 rpm. In extreme cases, motors with drive power up to 340 hp per inch grinding width are required for the grinding spindle drive. The high spindle speeds and large coolant flow rates result in extreme idling powers — e.g. for drill flute grinding they may be up to 15 hp.

Fig. 13—Thermal damage in workpiece increases steadily with increasing removal rate

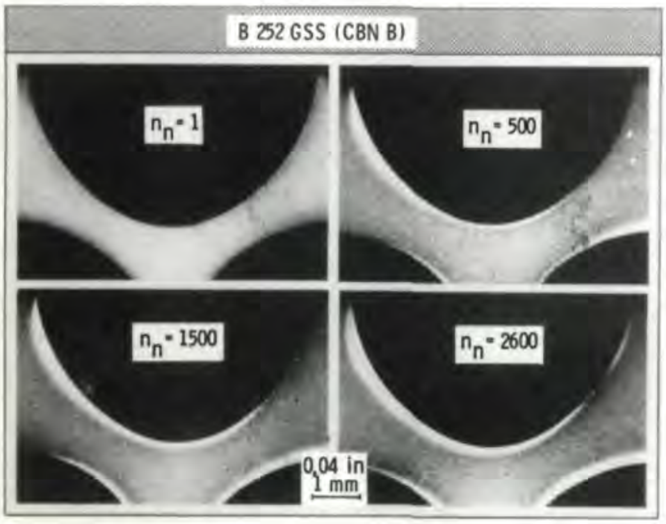

The high cutting speeds and forces necessitate high rigidity of the machine set-up for suppression of the increased process dynamics at high cutting speeds and forces, and extremely low-vibration grinding spindle motor systems. And balancing, which is not unproblematic at high wheel speeds, likewise plays an important role in the production of precision workpieces. Here it is advisible for hydro-dynamic balancing units to be built into the machine control system.

Optimization of coolant supply is necessary in order to combat the increased thermal loads. It is essential to use grinding oil as the coolant; copious amounts of coolant must be supplied under high pressure. The only way to achieve the high material removal rates required in the drill flute grinding tests, without causing thermal damage to the workpieces, was to enclose the grinding zone with a chamber sealed by the grinding wheel itself and the drill blank with the coolant forces into the chamber.

Automation of the trueing and sharpening process is essential, and the necessary components for this must be integrated into the machine. The development and design of these devices is particularly important, as wheel dressing is critical both for the working result and for the economy of the process. Fig. 14 shows some indications for the design of profiling and sharpening devices.

Economic Aspects

The economics of a CBN grinding process can only be assessed by an overall cost calculation, setting off the higher tool costs against the lower time costs.

The production costs per flute K_N may be approximated as follows:

$$K_N = k_{sLM} \left(\frac{V'_w}{Q'_w}\right) + \left(\frac{K_S}{n_d \cdot i_d}\right)$$

The left-hand side of the equation describes the labor and machine costs, while the right-hand side describes the tool costs, i.e. the grinding wheel costs. The symbols are defined as follows:

k_{sLM}: Labor and machine cost per hour
$\frac{V'_w}{Q'_w}$: Grinding time per flute
K_S : Grinding wheel costs
n_d : No. of flutes per trueing
i_d : No. of possible trueings per grinding wheel

Thus $n_d \cdot i_d$ is an expression for the total quantity of flutes that could be ground with the grinding layer used.

A comparison between resinoid bond and electroplating bond wheels shows major differences in the economics. (Fig. 15)

The production costs for resinoid bond wheels are about 50% lower. This is because the set-up time required for the electroplated bond CBN wheel is lower, and in addition, only a relatively small number of drill flutes can be ground without thermal damage to the workpiece. Thus, the proportional tool costs are considerably higher than for the resinoid bond CBN wheel.

With resinoid bond CBN wheels it is possible to reduce the production costs by about 20% by doubling the material removal rate from 6.3 in^3/in. min. to 12.6 in^3/in. min.; here

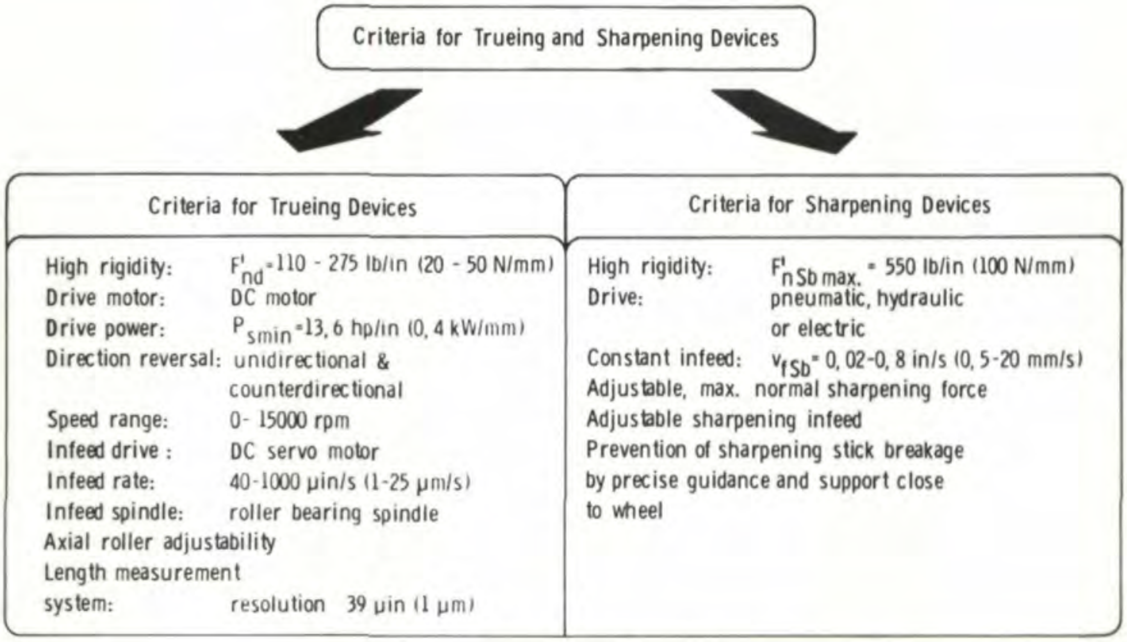

Fig. 14 – Design of trueing and sharpening devices

labor and machine cost per hour only plays a minor role. (Fig. 16)

At material removal rate of $Q'_w = 12.6$ in^3/in. min. it was only possible to grind 536 flutes before the tolerance limits were reached (2000 in). Since the wear was 5 times as high, but the production time was cut in half, and labor and machine costs were reduced, this became the dominant factors in production cost.

Fig. 15 – Resinoid bond wheels are more economical than electroplated wheels

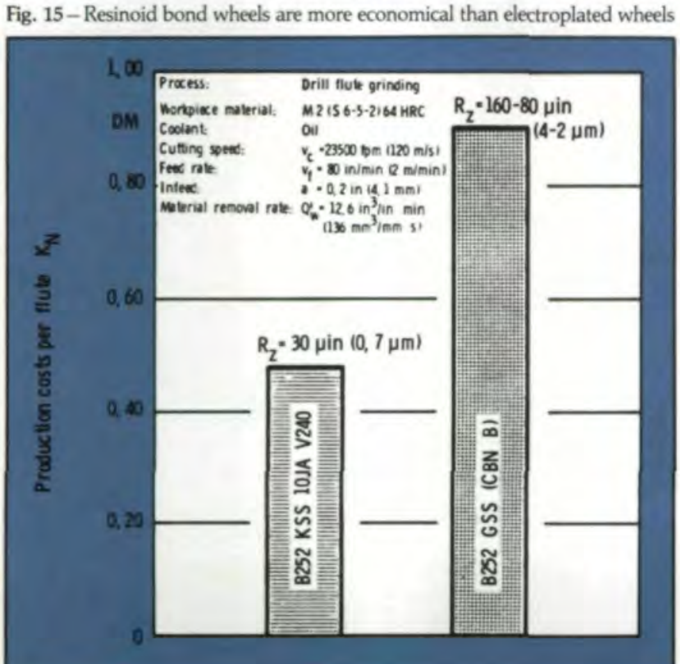

The results described above can be seen in the chart as shown on Fig. 17, which compares the best CBN grinding wheel with a typical corundum wheel. The higher cutting speed with CBN permits doubling of the material removal rates, whereby, the surface quality of the workpieces is even somewhat better than in corundum grinding. The grinding ration with CBN is about 20 times as high as with corundum.

This results in the time and tool costs shown; together with

(continued on page 48)

Fig. 16 – Doubling material removal rate reduced production cost by 20%

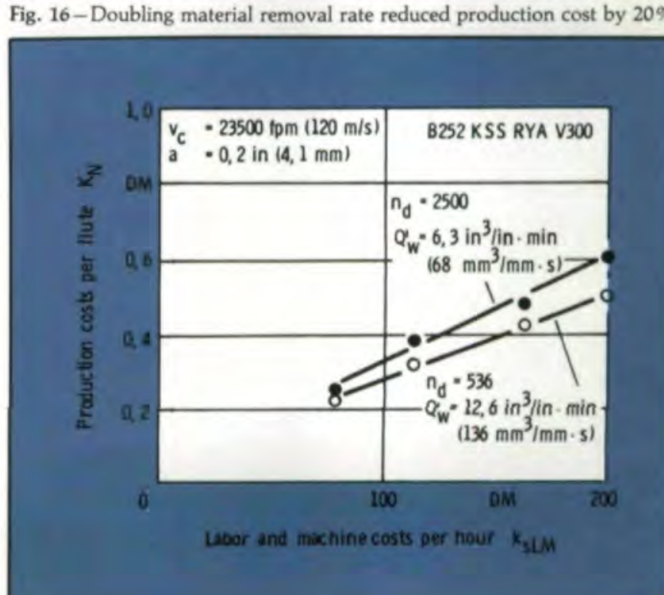

Optimum Number of Teeth for Span Measurement

by
J. R. Colbourne
University of Alberta
Edmonton, Alberta, Canada

Abstract

An expression is derived, giving the optimum number of teeth over which the span measurement should be made, for profile-shifted spur and helical gears.

Introduction

The span measurement is widely accepted as an accurate method for measuring gear tooth thickness. Once the span has been measured, for either spur or helical gears, the tooth thickness can be calculated without difficulty.[1] However, there is no simple expression, except in the case of spur gears with zero profile shift, giving the optimum number of teeth N′ over which the span should be measured.

When the span measurement is made, the contact between the tooth faces and the caliper jaws should be near the middle of the tooth profile. For gears with no profile shift, this means that the contact should be near the standard pitch circle. And for gears with profile shift e, the radius of the tip circle is generally extended by approximately the same amount e, so the contact should take place at distance e above the standard pitch circle. It is not possible to choose N′ so that the contact is always close to the required radius. For certain gears, one value of N′ may give contact points near the tips of the teeth, while, if N′ is reduced by 1, the contact points may be down near the fillets. However, it is obviously essential that the contact should always take place below the tooth tips and above the fillets, preferably with an adequate margin.

AUTHOR:

DR. JOHN COLBOURNE *obtained his Bachelor's degree in Mechanical Sciences in 1959 from Cambridge University, England, and his Ph.D. in Engineering Mechanics in 1965 from Stanford University, California. Since 1967, he has been employed as a Professor of Mechanical Engineering at the University of Alberta in Canada. His principal research interests have been the geometry and the tooth strength of spur and helical gears.*

Fig. 1—A base tangent section

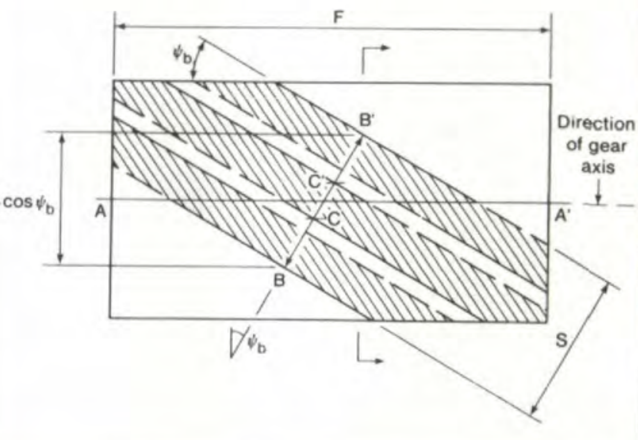

Relation Between the Span Measurement and the Tooth Thickness

Fig. 1 shows a base tangent section through the gear, touching the base cylinder along line AA′. The sections through each tooth are indicated by the shaded areas in the diagram. The upper edge of each tooth coincides with a generator above line AA′ and is, therefore, a straight line; while below line AA′, the tooth edge in the section is slightly curved. Similarly, the lower edge of each tooth is curved above line AA′, and it is straight below the line. Since the curved edges are very nearly straight, they are shown in the diagram as straight dotted lines. The span measurement is made between two points such as B and B′, on opposite sides of line AA′, and because B and B′ each lie on a straight tooth edge, the exact shape of the curved edges is of no significance. With the curved edges drawn as straight lines, the tooth edges all

Fig. 2—Transverse section through a contact point

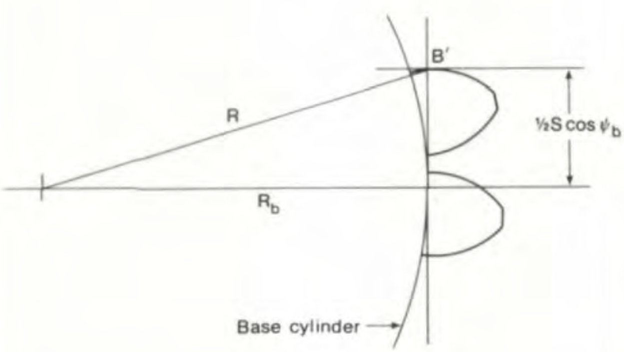

appear as parallel straight lines, making an angle with the gear axis equal to the base helix angle ψ_b, and the base tangent section is then identical with the developed base cylinder.

The length BB′ is made up of one tooth thickness measurement CC′, which crosses line AA′, and a number of pitch measurements such as BC. Since the base tangent section is the same as the developed base cylinder, at least as far as the solid lines are concerned, the length CC′ is equal to t_{nb}, the normal tooth thickness at the base cylinder, and the length BC is equal to the normal base pitch p_{nb}. Hence, if the span S is measured over N′ teeth, there are $(N'-1)$ lengths such as BC, and the span length is given by the following expression:

$$S = (N'-1)p_{nb} + t_{nb} \qquad (1)$$

This equation gives the value of t_{mb} immediately. The tooth thickness at the standard pitch cylinder can be found by converting first to the transverse tooth thickness at the base cylinder, and then to that at the standard pitch cylinder, in the usual manner.

$$t_{nb} = S - (N' - 1)p_{nb} \qquad (2)$$

$$t_{tb} = \frac{t_{nb}}{\cos \Psi_b} \qquad (3)$$

$$t_t = R_s \left(\frac{t_{tb}}{R_b} - 2 \text{ inv } \phi_s\right) \qquad (4)$$

$$t_n = t_t \cos \Psi_s \qquad (5)$$

In these equations, all quantitites with the subscript b are defined on the base cylinder, while the others are defined on the standard pitch cylinder, whose radius R_s is defined as follows:

$$R_s = \frac{N\, m_n}{2 \cos \Psi_s} \qquad (6)$$

where m_n is the normal module. The equations in this article are all given in terms of the normal and transverse modules m_n and m_t, but for those who prefer to use the corresponding diametral pitches, the final expression for the number of teeth to be spanned is given in both forms.

Optimum Span Length

The component of the span measurement perpendicular to the gear axis is $(S \cos \Psi_b)$, as we can see in Fig. 1. The transverse section through one of the measurement contact points is shown in Fig. 2, and the radius R of this point is found by Pythagoras' rule:

$$R^2 = R_b^2 + (\tfrac{1}{2}S \cos \Psi_b)^2 \qquad (7)$$

The profile shift e is related to the tooth thickness by the following two equations:

$$t_t = \tfrac{1}{2}\pi\, m_t + 2e \tan \phi_s \qquad (8)$$

$$t_n = \tfrac{1}{2}\pi\, m_n + 2e \tan \phi_c \qquad (9)$$

where ϕ_s and ϕ_c are the transverse and normal pressure angles of the gear at its standard pitch cylinder. For a gear with zero profile shift, the radius of the tip circle is generally approximately equal to $(R_s + m_n)$, while in a gear with profile shift e, this radius is usually increased by approximately e. Hence, if we want the contact to take place at a distance m_n below the tip circle, the radius R should be as close as possible to the radius of the standard pitch cylinder, plus the profile shift e.

$$R \cong R_s + e \qquad (10)$$

We substitute this expression for R into Equation (7), and replace the base cylinder radius R_b by $(R_s \cos \phi_s)$, in order

FAST, PRECISE, QUIET, CNC

Eliminates all manual functions

The new Star CNC horizontal hob sharpener is specially designed to bring the superior performance and longer life of Borazon® grinding wheels to this operation. The machine is capable of sharpening straight gash hobs up to 10"- diameter and 12"- long to AGMA "Class AA" tolerances.

Borazon® (CBN) is, next to diamond, the hardest abrasive known and has extremely high thermal strength compared to diamond. Successful CBN technique demands a stiff, rigid machine tool and intensive coolant flooding of the grinding zone. The Star Borazon® Hob Sharpener meets both these conditions due to its precise, rugged design and self contained coolant system with magnetic coolant cleaner and cartridge filter.

The CNC automatic cycle programming feature of this machine tool, a Star exclusive, eliminates all manual functions except for loading and unloading the hob. The machine is also very quiet (72 dba in cycle with approximately 68 dba background noise).

A number of CNC Borazon® Hob Sharpeners have been operating in automotive plants for some time with outstanding results. We offer fast delivery. Our machines are competitively priced. Service and engineering assistance is included. If interested, please write or phone for details.

*Trademark of General Electric Company, U.S.A.

...ORAZON* HOB SHARPENER

...xcept for loading and unloading

Lighted sharpening area is completely enclosed with sliding access door. (Grinding spindle assembly is easily accessible through sliding doors at rear of machine).

Operator's console has a grinding spindle load meter, a CRT screen and a keyboard for entering hob diameter, number of flutes, stock removal per rough and finish pass and number of passes, feed rate and right and left stroke limits. A CNC programmable controller is employed for sequence logic, feeding the grinding spindle slide, and positioning the hob spindle.

STARCUT SUPPLIED PRODUCTS AND SERVICES

Star Machine Tools
Standard and CNC Hob Sharpeners
Shaper Cutter Sharpeners
CNC Drill and Reamer Sharpeners
Keyseaters

Star Cutting Tools
Hobs
Form-Relieved Cutters
Gun Drills
Gun Reamers
Keyseat Cutters

Gold Star Coatings

Hurth Machine Tools
Standard & Automatic Keyway and Slot Milling Machines
Automatic Spline Shaft Milling Machines
CNC Gear Hobbing Machines
CNC Gear Shaving Machines
Gear Testing Machines
Shaving Cutter Grinding Machines
CNC Gear Tooth Chamfering Machines
Gear Deburring Machines
CNC Hard Gear Finishing Machines

TiN Coating Systems
Complete Turnkey Applications

PLANRING
Planning & Engineering
Flexible Machining Systems

Stieber Precision Clamping Tools

Since 1927
Star
STARCUT SALES, INC.
23461 Industrial Park Drive
Farmington Hills, MI 48024
313/474-8200 Telex 230-411

CIRCLE A-14 ON READER REPLY CARD

to obtain an expression for the optimum span measurement.

$$(\tfrac{1}{2}S \cos \Psi_b)^2 \cong (R_s + e)^2 - (R_s \cos \emptyset_s)^2 \qquad (11)$$

This equation is simplified by expanding the righthand side as a power series in (e/R_s), and retaining only the first two terms.

$$\tfrac{1}{2}S \cos \Psi_b = R_s \sin \emptyset_s + \frac{e}{\sin \emptyset_s} \qquad (12)$$

Number of Teeth to be Spanned

An expression for S was given in Equation (1). Before we make use of the expression, we put it in a more convenient form. The normal base pitch is expressed in terms of, first the transverse base pitch, then the transverse pitch at the standard pitch cylinder, and finally the transverse module. In a similar way, the tooth thickness t_{nb} is expressed in terms of t_{tb}, and then by means of Equations (4 and 8), in terms of the transverse module and the profile shift. We then obtain the following expression for S:

$$S = \cos \Psi_b \cos \emptyset_s \,[(N' - 1)\,\pi m_t + \tfrac{1}{2}\pi m_t$$
$$+ 2e \tan \emptyset_s + N m_t \operatorname{inv} \emptyset_s] \qquad (13)$$

We substitute this expression into Equation (12), and solve for N', the optimum number of teeth over which the span should be measured.

$$N' = \tfrac{1}{2} + \frac{N\emptyset_s}{\pi} + \frac{N}{\pi} \tan \emptyset_s \tan^2 \Psi_b + \frac{2e}{\pi\, m_n \tan \emptyset_c} \qquad (14)$$

The term $(N\emptyset_s/\pi)$ is derived from the function inv $\emptyset_s$ in the expression for S, and the angle $\emptyset_s$ must, therefore, be expressed in radians. Since it is common practice to use degrees in equations of this sort, the term can be replaced by $(N\emptyset_s^\circ/180)$.

In general, the value of N' given by Equation[14] is not an integer. It is obvious that the span measurement can only be made over an integer number of teeth, so in order to keep the measurement contact radius as close as possible to $(R_s + e)$, we choose N' as the integer closest to the value given by Equation.[14] Since the real value of N' may, therefore, differ by as much as 0.5 from the ideal value, it is important to determine whether the contact radius is still satisfactory.

For any particular gear, we can calculate the contact radius R by first finding the integer value N', then substituting this into Equation (13) to obtain the span length S, and finally using Equation[7] to find the corresponding value of R. We can, therefore, verify the validity of the expression for N' by calculating the contact radius R for a large number of gears. To be satisfactory, the radius R must always be less than the tip circle radius R_T, and greater than R_f, the radius of the true involute form circle which passes through the tops of the fillets.

The tip circle radius is chosen by the designer, but is generally close to the following value:

$$R_T = R_s + e + m_n \qquad (15)$$

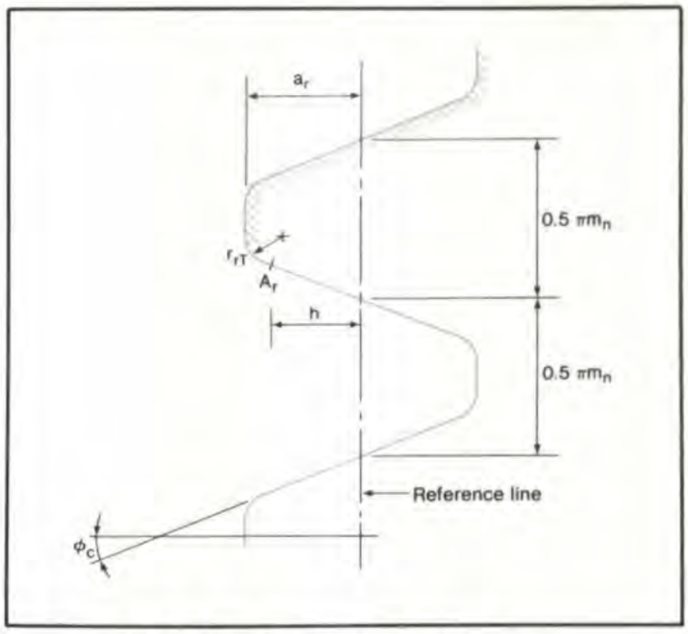

Fig. 3 – Normal section through the cutter

The radius of the true involute form circle depends on the type of cutter, and the dimensions of its teeth. For the present purpose, we will assume that the gear is cut by a rack cutter, with the normal tooth section shown in Fig. 3. The normal pitch is πm_n, and the normal pressure angle is $\emptyset_c$. The reference line is the line along which the tooth thickness is 0.5 πm_n, the addendum measured from this line is a_r, and the tooth tip radius is r_{rT}. If A_r is the end point of the straight section of the tooth profile, the distance h of point A_r from the reference line is given by the following expression:

$$h = a_r - r_{rT}\,(1 - \sin \emptyset_c) \qquad (16)$$

Fig. 4 shows the transverse section through the gear and

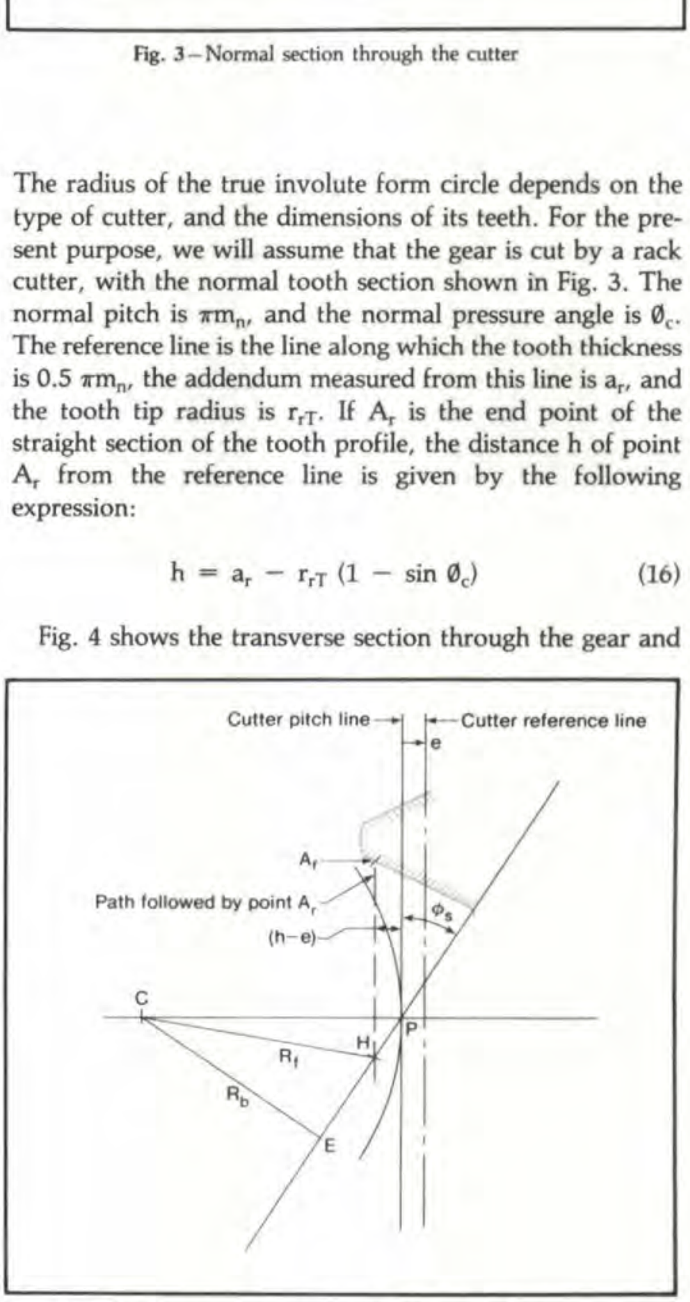

Fig. 4 – Transverse section through the gear and cutter

cutter during the cutting process. If the gear has a profile shift e, the cutter is offset by the same amount e, and the path followed by point A_r of the cutter is, therefore, a distance (h-e) from the pitch point. On the gear tooth, the end point of the fillet is cut by point A_r of the cutter, when A_r reaches the line of action. The radius R_f of the true involute form circle on the gear can then be found from the dimensions shown in Fig. 4:

$$R_f^2 = CE^2 + EH^2 = R_b^2 + [R_b \tan \emptyset_s - \frac{h - e}{\sin \emptyset_s}^2] \quad (17)$$

For the calculations described later in this article, it is assumed that the length h is equal to the normal module m_n.

If we simply wanted to be sure that we have a suitable value of N' for one particular gear, we could calculate the value of the contact radius R, and check R is less R_T and greater than R_f. In order to verify the general expression for N', we must carry out the same check for a very large number of gears, and it is essential to include all the worst possible cases. We define a measure ΔR of the error in N', as the difference between the actual and the ideal contact radii:

$$\Delta R = R - (R_s + e) \quad (18)$$

It is clear that the contact is only close to the tip circle or the true involute form circle in cases where the magnitude of ΔR is large.

We will consider gears with profile shift values between $-0.5\ m_n$ and $1.0\ m_n$. If we choose particular values for $\emptyset_c$, Ψ_s and N, and calculate the error ΔR for various values of e, we obtain a function such as the one shown in Fig. 5. The discontinuities occur each time there is a change in the value of N'. Since N' is the integer closest in value to the expression in Equation (14), the discontinuities in ΔR occur whenever this expression is exactly midway between two integers. The magnitude of ΔR reaches its largest values just before and just after each discontinuity, so these are the values of e at which the error must be calculated. In addition, it should also be calculated at $e = -0.5m_n$ and $e = 1.0\ m_n$.

The calculations just described have been carried out for various values of $\emptyset_c$, Ψ_s and N, with the following results.

Fig. 5 – Contact position error as a function of profile shift

The contact radius is satisfactory in all gears with small values of e, but for gears with large amounts of profile shift the value of N' given by Equation (14) is sometimes too large, and the contact points are then too close to the tooth tips. This occurs particularly in gears with a small number of teeth. In a few cases, the value of R is actually larger than R_T.

The reason for this large error is that the power series expansion used to derive Equation (12) is only accurate when (e/R_s) is small. The addition of a third term in the expansion makes the expression for N' very much more complicated, and does not significantly improve the accuracy. We, therefore, alter the expression in a manner that reduces the value of N' whenever e is large. We multiply the coefficient of e by the factor $[0.75 - (2/N)]$, which has the effect of halving the coefficient when N is 8, and reducing it by about 25% when N is large.

The number N' is then the integer closest to the following expression:

$$N' = \tfrac{1}{2} + \frac{N\emptyset_s^\circ}{180} + \frac{N}{\pi} \tan \emptyset_s \tan {}^2\Psi_b + \frac{2e[0.75-(2/N)]}{\pi m_n \tan \emptyset_c} \quad (19)$$

Since a span measurement over one tooth is impossible, the minimum value to be used for N' is 2, even in cases where the value of the expression in Equation (19) is less than 1.5. The equation can also be expressed in terms of the normal diametral pitch P_{nd}, if the ratio (e/m_n) is replaced by the quantity (eP_{nd}).

There is no theoretical basis for the modification made to the coefficient of e. However, the new expression for N' has been tested in the manner described earlier, and has been found to work very well. The calculations were carried out for normal pressure angles of 14.5°, 15°, 17.5°, 20°, 22.5° and 25°, helix angles of all integers from 0° to 45°, and all tooth numbers from 8 to 160.

In the cases considered, the minimum distance between the contact point and the tooth tip was 0.383 m_n, while the minimum distance between the contact point and the top of the fillet was 0.272 m_n. With the ranges of $\emptyset_c$, N and e values that were studied, it is clear that some of the gears would be undercut. In order to avoid making calculations for gears that would never exist in practice, the calculation was discontinued in cases where the ideal contact radius $(R_s + e)$ was less then R_b. For the remaining undercut gears, the radius of the contact point was compared with the undercut circle radius, which can be found by trial and error.[2] The minimum distance between the two circles was found to be 0.133 m_n.

We have shown that, for gears with standard length teeth, there is always adequate clearance between the measurement contact point and the tooth tip. Equation (19) can, therefore, also be used to calculate the optimum value of N' for stub-toothed gears. In addition, the clearance is generally sufficient to allow the span measurement of gears with tip relief. The contact takes place either on the involute part of the tooth face, or on a part where the tooth thickness is not significantly altered by the tip relief. The only exceptions occur in gears with a very small number of teeth, for which the span measurement is made over only two teeth. In some of these gears, the contact point may lie well within the tip-relieved part of the tooth face. It is, therefore, advisable for gears with N' equal to 2, to check the value of R at which the measurement contact is made. If the tooth thickness at this radius is seriously reduced by the tip relief, then the span measurement should not be used.

Examples

The first example deals with the inspection measurement of a typical helical gear, and shows how Equations (19, 13 and 7) are used to calculate the number of teeth to be spanned, the corresponding span length, and the radius of the measurement contact point.

Given: $m_n = 10$ mm, $N = 35$, $\emptyset_c = 20°$, $\Psi_s = 30°$,

$$e = 3.000 \text{ mm}$$

$$\text{Then: } R_s = \frac{Nm_n}{2\cos\Psi_s} = 202.073$$

$$m_t = \frac{m_n}{\cos\Psi_s} = 11.547$$

$$\tan\emptyset_s = \frac{\tan\emptyset_c}{\cos\Psi_s} \qquad \emptyset_s = 22.796°$$

$$R_b = R_s\cos\emptyset_s = 186.289$$

$$\tan\Psi_b = \frac{R_b\tan\Psi_s}{R_s} \qquad \Psi_b = 28.024°$$

N' = Integer closest to (6.6225) = 7

S = 201.312 mm

R = 206.394 mm

$R - (R_s + e) = 1.322$ mm

The second example deals with a spur gear, and was chosen to illustrate that we obtain a suitable measurement radius when N' is calculated from Equation (19), but that the earlier expression given by Equation (14) sometimes gives an impractical measurement radius.

Given: $m_n = 10$ mm, $N =$, $\emptyset_c = 14.5°$,
$\Psi_s = 0$, $e = 9.000$ mm;

$$\text{Then: } R_s = \frac{Nm_n}{2} = 60.000$$

$m_t = m_n$, $\emptyset_s = \emptyset_c$, $\Psi_b = 0$
$R_b = R_s\cos\emptyset_s = 58.089$

Using Eq. (19), N' = Integer closest to (2.7590) = 3
$S = 81.189$ mm
$R = 70.868$ mm
$R - (R_s + e) = 1.868$ mm

Using Eq. (14), N' = Integer closest to (3.6821) = 4
$S = 111.604$ mm
$R = 80.549$ mm
$R - (R_s + e) = 11.549$ mm
$R_T = R_s + e + m_n = 79.000$ mm
i.e. $R > R_T$

References

1. M. F. SPOTTS, "Special Calculations for Spur and Helical Gears", Chapter 7 in the "Gear Handbook", edited by D. W. Dudley, McGraw-Hill, 1962.
2. J. R. COLBOURNE, "The Design of Undercut Gears", ASME paper 80-C2/DET-67, presented at the Century 2 International Power Transmissions and Gearing Conference, San Francisco, 1980.

This article was previously presented at the AGMA Fall Technical Meeting, Paper No. 85FTM9.

Effect of Shot Peening on Surface Fatigue Life of Carburized and Hardened AISI 9310 Spur Gears

by
Dennis P. Townsend and Erwin V. Zaretsky
NASA Lewis Research Center
Cleveland, Ohio

Summary

Gear surface fatigue endurance tests were conducted on two groups of 10 gears each of carburized and hardened AISI 9310 spur gears manufactured from the same heat of material. Both groups were manufactued with standard ground tooth surfaces. The second group was subjected to an additional shot-peening process on the gear tooth surfaces and root radius to produce a residual surface compressive stress. The gear pitch diameter was 8.89 cm (3.5 in.). Test conditions were a gear temperature of 350 K (170°F), a maximum Hertz stress of 1.71×10^9 N/m^2 (248 000 psi), and a speed of 10 000 rpm.

The shot-peened gears exhibited pitting fatigue lives 1.6 times the life of the standard gears without shot peening. Residual stress measurements and analysis indicate that the longer fatigue life is the result of the higher compressive stress produced by the shot peening. The life for the shot-peened gear was calculated to be 1.5 times that for the plain gear by using the measured residual stress difference for the standard and shot-peened gears. The measured residual stress for the shot-peened gears was much higher than that for the standard gears.

Introduction

Shot peening has long been used as a method for improving the bending strength of gear teeth.[1-3] However, shot peening has not been considered as a means of extending the surface fatigue life of gears. In essence, shot peening induces a residual compressive stress below the surface of the gear tooth. Studies of residual stresses in rolling-element bearings have shown that increased residual compressive stress will increase rolling-element (surface) fatigue life.[4-5] There is always a need to improve the surface fatigue life of aircraft gears, especially in helicopter and V/STOL aircraft.

The objectives of the research reported herein were (1) to investigate the effects of shot peening of gear teeth on the surface fatigue life of standard ground, case-carburized, and hardened AISI 9310 spur gears, (2) to compare the life of shot-peened gears to that of non-shot-peened gears manufactured with the same material and specifications, and (3) to determine the residual stress produced by shot peening and its effect on the surface fatigue life.

To accomplish these objectives, 20 spur gears were manufactured from a consumable-electrode-vacuum-melted single heat of AISI 9310 material. Ten of these gears were shot peened after finish grinding. The gear pitch diameter was 8.89 cm (3.5 in.). Both the shot-peened and non-shot-peened gears were then tested to fatigue by surface pitting under identical test conditions. These test conditions included a gear temperature of 350 K (170°F), a maximum Hertz stress of 1.71×10^9 N/m^2 (248 000 psi), and a speed of 10 000 rpm.

Apparatus, Specimens, and Procedure

Gear Test Apparatus

The gear fatigue tests were performed

AUTHORS:

DR. ERWIN V. ZARETSKY *has been a member of the research staff of the NASA Lewis Research Center since 1957 where he is Chief Engineer for Structures. He was head of the NASA Bearing, Gearing and Transmission Section and was manager of the NASA Helicopter Transmission System Technology Program. Zaretsky is author or co-author of over 125 technical papers, books, and articles in the field of bearings, gears and lubrication technology. He is a Licensed Professional Engineer in Ohio and has been admitted to the Bars of Ohio and Illinois as well as the Federal Bar. Zaretsky has chaired several national committees for the ASME and was a Director of the Cleveland Society of Professional Engineers and is a former Chairman of the Cleveland Section of ASME. The Lubrication Division of the ASME honored him in 1972, by bestowing upon him their Distinguished Service Award. In 1979, he was further honored by the ASME when he was made Fellow of the Society. Dr. Zaretsky has a BSME from the Illinois Institute of Technology and a Doctor of Law Degree from Cleveland State University.*

MR. DENNIS P. TOWNSEND *is the Manager of the Gear Research Program for Advanced Aircraft Applications at the NASA Lewis Research center. He directs and conducts research on gear lubrication, gear materials, and gear design. He has authored or co-authored over 54 NASA technical society publications. Townsend holds a BS in Mechanical Engineering from the University of West VA. He served with the ASME Design Division as Chairman of the Power Transmission and Gearing Committee from 1978 to 1983, and he was Papers Review Chairman and Associate Editor of the journal for two years. He is now a member of the ASME Design Engineering Division Executive Committee.*

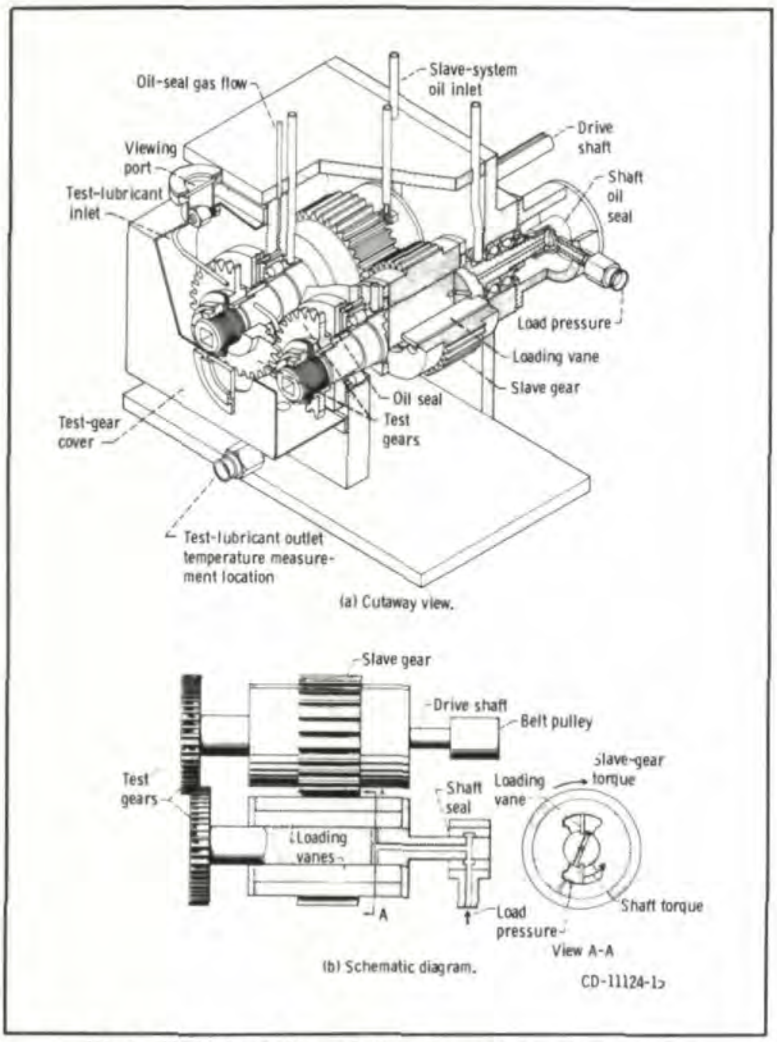

Fig. 1—NASA Lewis Research Center's gear fatigue test apparatus.

TABLE I.
SHOT-PEENING
SPECIFICATION

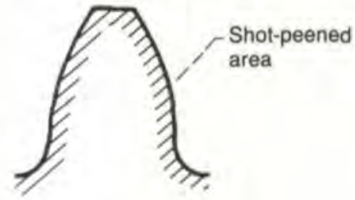

Specification	MIL-S-131658 BPS FW 4409
Shot size	.070
Shot type	Cast steel
Intensity (height of Almen strip, type A), mm (in.)	0.18 to 0.23 (0.007 to 0.009)
Coverage (sides and root only), percent	200

TABLE II.
NOMINAL CHEMICAL
COMPOSITION OF CVM AISI
9310 GEAR MATERIAL

Element	Composition, wt%
C	0.10
Mn	.63
Si	.27
Ni	3.22
Cr	1.21
Mo	.12
Cu	.13
P	.005
S	.005

in the NASA Lewis Research Center's gear test apparatus (Fig. 1). This test rig uses the four-square principle of applying the test gear load, so that the input drive only needs to overcome the frictional losses in the system.

A schematic of the test rig is shown in Fig. 1(b). Oil pressure and leakage flow are supplied to the load vanes through a shaft seal. As the oil pressure is increased on the load vanes inside the slave gear, torque is applied to the shaft. This torque is transmitted through the test gears back to the slave gear, where an equal, but opposite torque is maintained by the oil pressure. This torque on the test gears, which depends on the hydraulic pressure applied to the load vanes, loads the gear teeth to the desired stress level. The two identical test gears can be started under no load, and the load can be applied gradually, without changing the running track on the gear teeth.

Separate lubrication systems are provided for the test gears and the main gearbox. The two lubrication systems are separated at the gearbox shafts by pressurized labyrinth seals. Nitrogen is the seal gas. The test gear lubricant is filtered through a 5-μm-nominal fiberglass filter. The test lubricant can be heated electrically with an immersion heater. The temperature of the heater skin is controlled to prevent overheating the test lubricant.

A vibration transducer mounted on the gearbox is used to automatically shut off the test rig when a gear surface fatigue occurs. The gearbox is also automatically shut off if there is a loss of oil flow to either the main gearbox or the test gears, if the test gear oil overheats, or if there is a loss of seal gas pressurization.

The belt-driven test rig can be operated at several fixed speeds by changing pulleys. The operating speed for the tests reported herein was 10 000 rpm.

Test Materials

The test gears were manufactured from consumable-electrode-vacuum-melted (CVM) AISI 9310 steel from the same heat of material. Both sets of gears were case hardened to a case hardness of Rockwell C58 and a case depth of 0.97 mm (0.038 in.). The nominal core hardness was Rockwell C40. One set of the gears was shot peened, after finish grinding, on the tooth root and the tooth profile according to the specifications given in Table I. The chemical composition of the material is given in Table II. Both sets of gears were case carburized and heat treated in accordance with the heat treat-

Fig. 2 – Photomicrographs of case and core for standard and shot-peened spur gears.

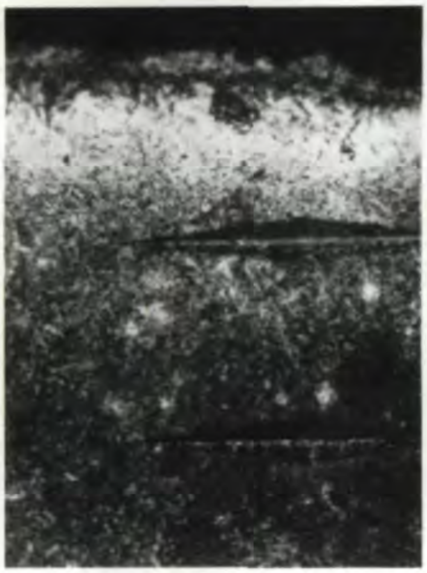

(a) Standard gear case.

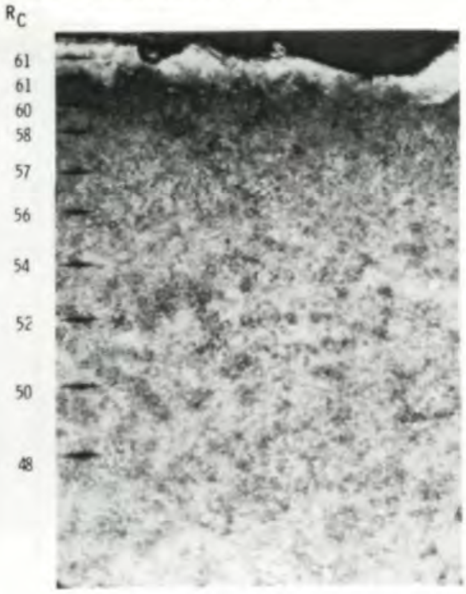

(b) Standard gear core.

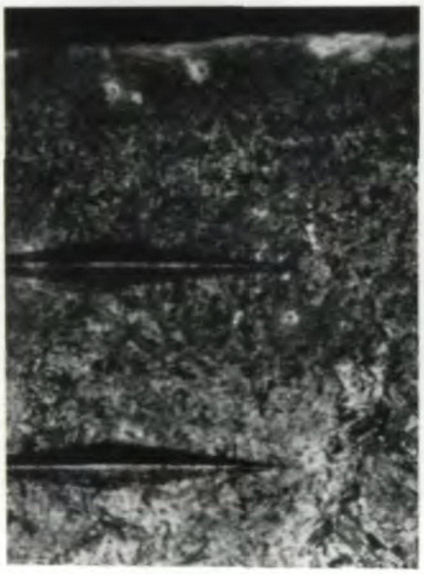

(c) Shot-peened gear case.

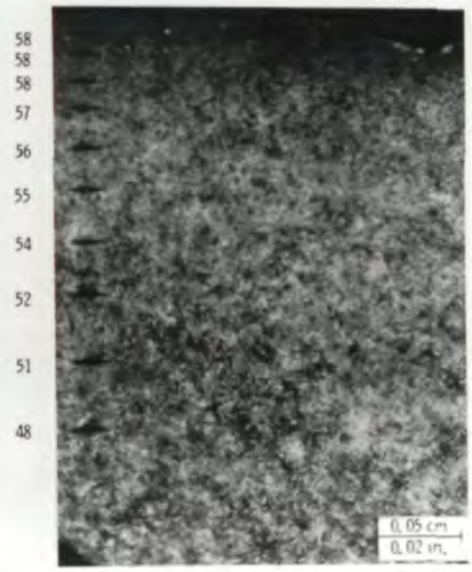

(d) Shot-peened gear core.

Fig. 3 – Surface finish of standard ground and shot-peened gears.

ment schedule of Table III. Fig. 2 is a photomicrograph of an etched and polished gear tooth surface showing the case microstructure of the AISI 9310 material.

Test Gears

Dimenions of the test gears are given in Table IV. All gears have a nominal surface finish on the tooth face of 0.406 μm (16 μin.) rms and a standard 20° involute profile with tip relief. Tip relief was 0.0013 cm (0.0005 in.), starting at the highest point of single-tooth contact. Surface traces of the standard gear and the shot-peened gear are shown in Fig. 3.

Test Lubricant

All gears were lubricated with a single batch of synthetic paraffinic oil. The physical properties of this lubricant are summarized in Table V. Five percent of an extreme-pressure additive, designated Lubrizol 5002 (partial chemical analysis given in Table V), was added to the lubricant.

Test Procedure

After the test gears were cleaned to

TABLE III. - HEAT TREATMENT FOR AISI 9310

Step	Process	Temperature		Time, hr
		K	°F	
1	Preheat in air	----	----	------
2	Carburize	1172	1650	8
3	Air cool to room temperature	----	----	------
4	Copper plate all over	----	----	------
5	Reheat	922	1200	2.5
6	Air cool to room temperature	----	----	------
7	Austenitize	1117	1550	2.5
8	Oil quench	----	----	------
9	Subzero cool	180	-120	3.5
10	Double temper	450	350	2 each
11	Finish grind	----	----	------
12	Stress relieve	450	350	2

TABLE IV. - SPUR GEAR DATA

[Gear tolerance per ASMA class 12.]

Number of teeth	28
Diametral pitch	8
Circular pitch, cm (in.)	0.9975 (0.3927)
Whole depth, cm (in.)	0.762 (0.300)
Addendum, cm (in.)	0.318 (0.125)
Chordal tooth thickness (reference), cm (in.)	0.485 (0.191)
Pressure angle, deg	20
Pitch diameter, cm (in.)	8.890 (3.500)
Outside diameter, cm (in.)	9.525 (3.750)
Root fillet, cm (in.)	0.102 to 0.152 (0.04 to 0.06)
Measurement over pins, cm (in.)	9.603 to 9.630 (3.7807 to 3.7915)
Pin diameter, cm (in.)	0.549 (0.216)
Backlash reference, cm (in.)	0.0254 (0.010)
Tip relief, cm (in.)	0.001 to 0.0015 (0.0004 to 0.0006)
Tooth width, cm (in.)	0.635 (0.25)

TABLE V. - PROPERTIES OF SYNTHETIC PARAFFINIC OIL

Additive	[a]Lubrizol 5002
Kinematic viscosity, cm^2/sec (cS) at-	
244 K (-20° F)	2500×10^{-2} (2500)
311 K (100° F)	31.6×10^{-2} (31.6)
372 K (210° F)	5.7×10^{-2} (5.7)
477 K (400° F)	2.0×10^{-2} (2.0)
Flashpoint, K (°F)	508 (455)
Fire point, K (°F)	533 (500)
Pour point, K (°F)	219 (-65)
Specific gravity	0.8285
Vapor pressure at 311 K (100° F), mm Hg (or torr)	0.1
Specific heat at 311 K (100° F), J/kg K (Btu/lb °F)	676 (0.523)

[a]Additive, Lubrizol 5002 (5 vol%); content of additive: phosphorus, 0.6 wt%; sulfur, 18.5 wt%.

TABLE VI. - FATIGUE RESULTS WITH AISI 9310 STANDARD AND SHOT-PEENED TEST GEARS

Gears	10-Percent life, cycles	50-Percent life, cycles	Slope	Failure index[a]	Confidence number,[b] percent
Standard	19×10^6	46×10^6	2.1	18/18	--
Shot peened	30	68	2.3	24/24	83

[a]Indicates numbers of failures out of total number of tests.
[b]Probability, expressed as a percentage, that the 10-percent life with the baseline AISI 9310 gears is either less than, or greater than, that of the particular lot of gears being considered.

remove the preservative, they were assembled on the test rig. The 0.635 cm (0.25 in.) wide test gears were run in an offset condition with a 0.30 cm (0.12 in.) tooth-surface overlap to give a load surface on the gear face of 0.28 cm (0.11 in.), thereby, allowing for the edge radius of the gear teeth. If both faces of the gears were tested, four fatigue tests could be run for each set of gears. All tests were run in at a pitch-line load of 1225 N/cm (700 lb/in.) for 1 hour, which gave a maximum Hertz stress of 0.756×10^9 N/m^2 (111 000 psi). The load was then increased to 5784 N/cm (3305 lb/in.), which gave a pitch-line maximum Hertz stress of 1.71×10^9 N/m^2 (248 000 psi). At this pitch-line load the tooth root bending stress would be 0.21×10^9 N/m^2 (30 000 psi), if plain bending were assumed. However, because there was an offset load, an additional stress was imposed on the tooth bending stress. Combining the bending and torsional moments gave a maximum stress of 0.26×10^9 N/m^2 (37 000 psi). This bending stress does not include the effects of tip relief, which would also increase the bending stress.

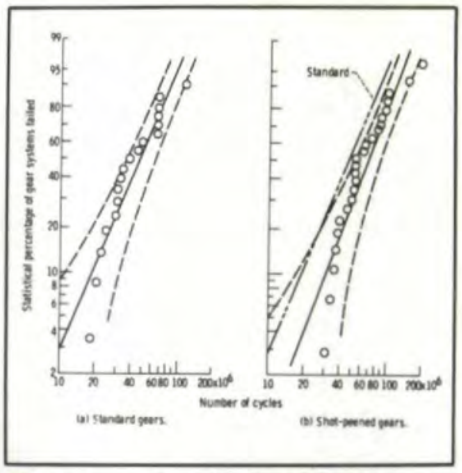

Fig. 4 – Comparison of surface (pitting) fatigue lives of standard ground and shot-peened carburized and hardened CVM AISI 9310 steel spur gears. Speed, 10 000 rpm; lubricant, synthetic paraffinic oil; gear temperature, 350 K (170° F); maximum Hertz stress, 1.7×10^9 N/m^2 (248 000 psi).

Operating the test gears at 10 000 rpm gave a pitch-line velocity of 46.55 m/sec (9163 ft/min). Lubricant was supplied to the inlet mesh at 800 cm^3/min at 319 ± 6 K (116° ± 10°F). The lubricant outlet temperature was nearly constant at 350 ±3 K (170° ±5°F). The tests ran continuously (24 hr/day) until they were automatically shut down by the vibration detection transducer, located on the gearbox adjacent to the test gears. The lubricant circulated through a 5-μm fiberglass filter to remove wear particles. After each test, the lubricant and the filter element were discarded. Inlet and outlet oil temperatures were continuously recorded on a strip-chart recorder.

The pitch-line elastohydrodynamic

VIEWPOINT (continued from page 6)

hob manufacturing units in India and I am also doing consultancy work for gear design and manufacturing problems. I have been working in this field for the past fifteen years.

I would be extremely grateful if you could add my name along with the list of qualified people who could get the magazine.

We would also like to have all the earlier issues published.

S. V. Shanmugam
Chowgule Matrix Hobs Ltd
India

We run a machine shop under UNDP assistance for training and production of spare parts for small scale industries. We would like to subscribe to your magazine GEAR TECHNOLOGY.

Demrew Metaferia
National Project Officer
Addis Ababa, Ethiopia

I have been asked by several members of our research staff to approach you for the above journal.

Research is an important aspect of our work and the journal would reach a substantial number of people who have a direct influence on purchasing policies of this Department and of "clients". It would also introduce manufacturers' names to our undergraduates and postgraduate students for their future use.

Hilary M. Pickett
Librarian
Cambridge University
England

Many thanks for your letter. I must confess that the first issue of "GEAR TECHNOLOGY" was well received. In fact, someone pinched my copy. I, therefore, enclose the appropriate draft for one year's subscription plus the necessary addition for the five issues you will already have completed by the time this letter arrives.

Ronald Cowee
Gear Machines & Tools Pty. Ltd
Marrickville, Australia

We received a complimentary copy of your publication; GEAR TECHNOLOGY at the Fourth International Power Transmission and Gearing conference of the ASME. We found it very interesting. We would like to receive a regular subscription.

Denis St-Georges
Project Engineer
Commission de transport
de la Communaute urbaine
de Montreal
Canada

(EHD) film thickness was calculated by the method of Reference 6. It was assumed, for this film thickness calculation, that the gear temperature at the pitch line was equal to the outlet oil temperature and that the inlet oil temperature to the contact zone was equal to the gear temperature, even though the inlet oil temperature was considerably lower. It is possible that the gear surface temperature was even higher than the outlet oil temperature, especially at the end points of sliding contact. The EHD film thickness for these conditions was computed to be 0.33 μm (13 μin.), which gave an initial ratio of film thickness to composite surface roughness h/σ of 0.55 at the 1.71×10^9 N/m^2 (248 000 psi) pitch-line maximum Hertz stress.

Results and Discussion

Gears manufactured from CVM AISI 9310 material were tested in pairs until failure or for 500 hours. One-half of the gears were shot peened on the tooth root and profile. Nineteen tests were run with standard-finish ground test gears, and 24 tests were run with standard-finish ground gears that had been shot peened. Test results were analyzed by considering the life of each pair of gears as a system.

Surface (pitting) fatigue results for the standard-finish AISI 9310 gears are shown in Fig. 4(a). These data were analyzed by the method of Reference 7. The 10- and 50-percent fatigue lives were 18.8×10^6 and 46.1×10^6 stress cycles (31.3 and 76.8 hr), respectively. These results are summarized in Table VI. The failure index (i.e., the number of fatigue failures out of the number of sets tested) was 18 out of 18. A typical fatigue spall is shown in Fig. 5(b). A cross section of a typical fatigue spall is shown in Fig. 5(a). The surface pitting failure occurs slightly below the pitch line in the area of highest Hertz stress and is of subsurface origin.

Pitting fatigue life results for the gears that were shot peened are shown in Fig. 4(b). The failure index was 24 out of 24. A typical fatigue spall for the shot-peened gears is shown in Fig. 6(a). A cross section of a typical fatigue spall for the shot-peened gears is shown in Fig. 6(b). The 10- and 50-percent surface pitting fatigue lives were 30.1×10^6 and 67.5×10^6 stress cycles (50.3 and 112.6 hr), respectively. These results are summarized in Table VI. The shot-peened gears exhibited a 10-percent fatigue life of 1.6 times that of the standard ground AISI 9310 gears. The confidence number for the difference in life was 83 percent. The mean life ratio for the shot-peened over the standard AISI 9310 gears was 1.5, with a confidence number of 98 percent. The confidence number indicates the percentage of time the relative lives of the material will occur in the same order. The 90-percent confidence bands for the standard ground and shot-peened AISI 9310 test gears are shown in Fig. 4. A confidence number of 95 percent is equivalent to a 2σ confidence level.

It is well known that shot peening produces residual subsurface stresses in steel in addition to the residual stresses produced by case carburizing, hardening, and grinding. It was theorized that the additional residual stresses induced by shot peening should account for the increased life of the shot-peened gears. Therefore, two shot-peened and untested

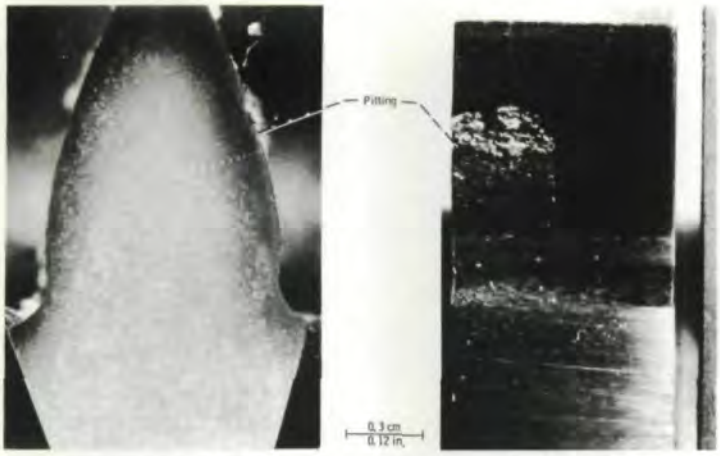

(a) Cross section of typical fatigue spall (b) Typical fatigue spall.

Fig. 5—Fatigue spall for standard ground gear.

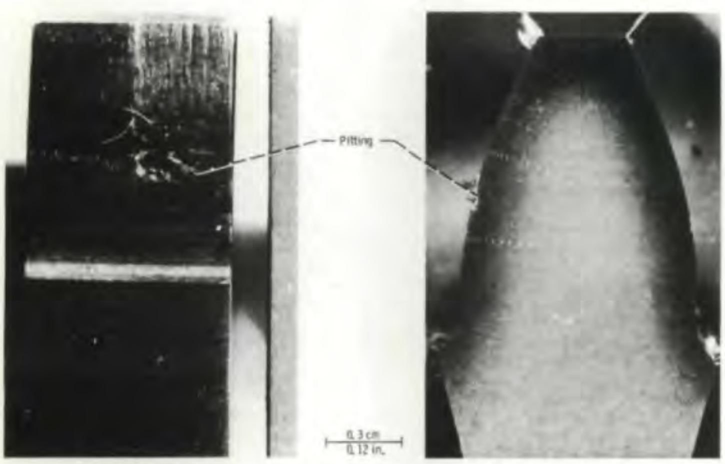

(a) Typical fatigue spall. (b) Cross section of typical fatigue spall

Fig. 6—Fatigue spall for shot-peened gear.

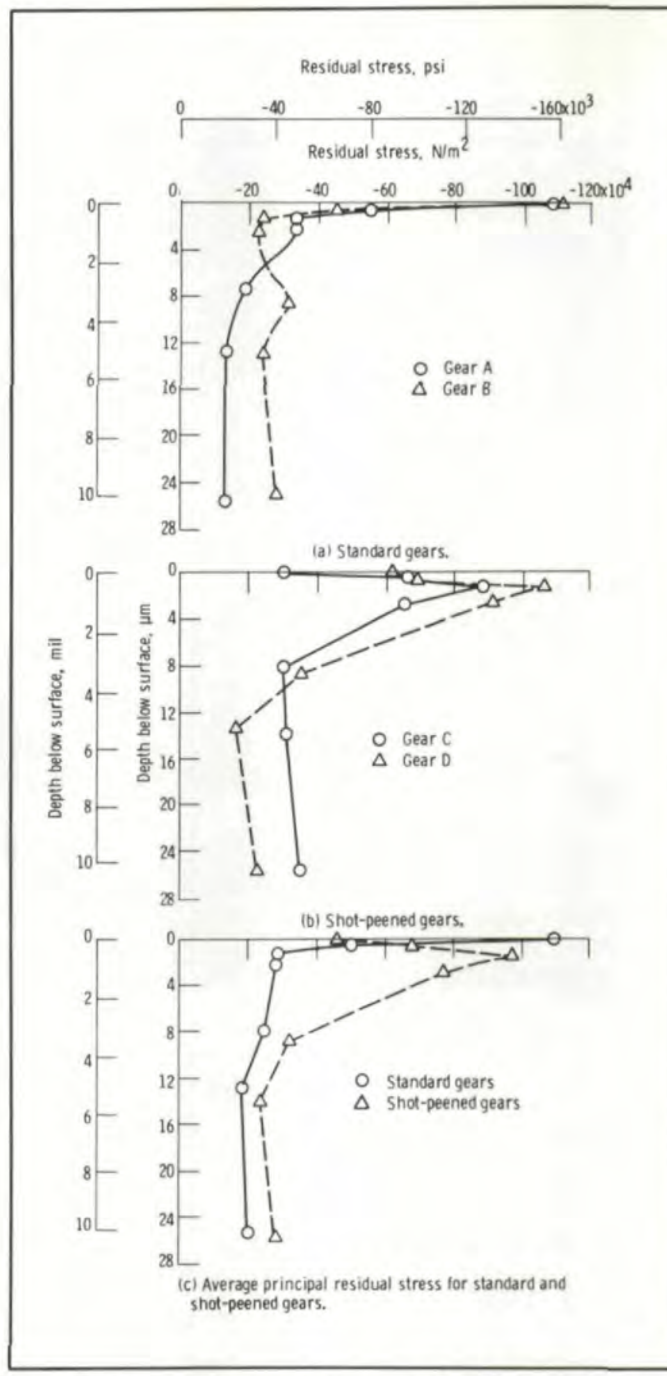

Fig. 7—Principal residual stress as a function of depth below the surface of carburized, hardened, ground and untested AISI 9310 steel spur gear teeth.

gear teeth and two standard ground and untested gear teeth were subjected to X-ray diffraction residual stress measurements to determine the magnitude of these residual stresses. Residual stress measurements were made near the pitch point at the surface and at nominal subsurface depths of 5, 13, 25, 76, 127, and 254 μm (0.2, 0.5, 1.0, 3, 5, and 10 mil).

Material was removed for subsurface measurement by electropolishing in a sulphuric-phosphoric-chromic acid electrolyte in order to minimize possible alteration of the subsurface residual stress distribution as a result of material removal. All data obtained as a function of depth were corrected for the effects of the penetration of the radiation employed for residual stress measurement into the subsurface stress gradient and for stress relaxation, which occurred as a result of material removal. The method used for the X-ray stress measurements and the calibration procedures used are described in References 8 and 9.

Fig. 7(a) shows two corrected X-ray diffraction residual stress measurements as a function of depth below the surface for the standard ground AISI 9310 gear teeth that had not been shot peened or tested. The high compressive stress on the surface of the gear tooth is the result of grinding and has a very shallow depth that has very little effect on the surface durability of the gear. The lower compressive stress, which has much greater depth, is from the case carburizing and hardening of the gear tooth surface. This compressive residual stress has a definite beneficial effect on surface fatigue and bending fatigue life.

Fig. 7(b) contains two plots of corrected X-ray diffraction residual stress measurements as a function of depth below the surface in the ground and shot-peened AISI 9310 gear teeth that had not been tested. The high grinding compressive stress on the surface was reduced. A hook in the curve shows a high compressive stress 1.3 μm (0.5 mil) below the surface as a result of the shot peening. The compressive stress at greater depths below the surface was also increased as a result of the shot peening. It is the increased compressive stress at the greater depths that has the major effect on the surface fatigue life. The depth to the maximum shear stress for the load conditions reported herein was 178 μm (7 mil).

Fig. 7(c) contain plots of the average of the two X-ray residual stress measurements as a function of depth below the surface for both the standard ground and shotpeened gears. This Fig. shows the average increase in the residual compressive stress due to shot peening. At the maximum shear stress depth of 178 μm (7 mil) the average residual compressive stress was increased from 0.186×10^9 N/m^2 (27 000 psi) in the standard ground AISI 9310 gear to 0.26×10^9 N/m^2 (37 700 psi) in the ground and shot-peened AISI 9310 gear. From equation (A11), taken from the analysis given in the appendix for maximum shear stress and residual stress,

$$(\tau_{\max})_r = -3.15 \times 10^6 \left(\frac{P_N}{L S_{\max} R} \right) - \frac{1}{2} S_{ry}$$

where

$R = 7.62$ mm (0.3 in.)

$S_{\max} = 1.71 \times 10^9$ N/m^2 (248 000 psi)

$\frac{P_N}{L} = 578\ 375$ N/m (3305 lb/in)

Therefore for peened gears, in SI units,

$$(\tau_{\max})_r = -21.74 \times 10^9 \frac{578\ 375}{0.00762 \times 1.71 \times 10^9} - \frac{1}{2} (0.26 \times 10^9) = -0.835 \times 10^9$$

in U.S. customary units,

$$(\tau_{\max})_r = -3.15 \times 10^6 \frac{3305}{0.3 \times 248\ 000} - \frac{1}{2} (-37\ 000)$$

$$= -121\ 080$$

And for standard gears, in SI units,

$$(\tau_{\max})_r = -21.74 \times 10^9 \frac{578\ 375}{0.00762 \times 1.71 \times 10^9} - \frac{1}{2} (0.186 \times 10^9) = -0.872 \times 10^9$$

in U.S. customary units,

$$(\tau_{\max})_r = -3.15 \times 10^6 \frac{3305}{0.3 \times 248\ 000} - \frac{1}{2} (-27\ 000) = -126\ 430$$

The surface fatigue life[10] for gears is inversely proportional to the maximum shear stress to the ninth power. The calculated life ratio from measured residual stress is therefore

$$\frac{L_{10_p}}{L_{10_s}} = \left[\frac{(\tau_{\max})_{rs}}{(\tau_{\max})_{rp}} \right]^9 = \left(\frac{0.872 \times 10^9}{0.835 \times 10^9} \right)^9 = 1.5$$

This calculated ratio of the fatigue life of the shot-peened gears to that of the standard gear compares favorably with the experimental fatigue life ratio of 1.6.

Summary of Results

Gear surface fatigue endurance tests were conducted on two groups of carburized and hardened AISI 9310 steel spur gears manufactured from the same heat of material. Both groups were manufactured with a standard ground tooth surface. One group was subjected to an additional shot-peening process on the gear tooth surface and root radius to produce a residual compressive surface stress. The gear pitch diameter was 8.89 cm (3.5 in.). Test conditions were a gear temperature of 350 K (170° F), a maximum Hertz stress of 1.71×10^9 N/m^2 (248 000 psi), and a speed of 10 000 rpm. The lubricant was a synthetic paraffinic oil with an additive package.

The following results were obtained:

1. The 10-percent surface (pitting) fatigue life of the shot-peened gears was 1.6 times that for the standard test gears that were not shot peened. This was shown to be statistically significant.
2. The calculated 10-percent surface (pitting) fatigue life for the shot-peened gears determined from measured residual subsurface stress was 1.5 times that for the standard gears that were not shot peened.
3. Measured residual stresses for the standard and shot-peened gears show an increase of 40 percent for the shot-peened gears over the standard gears at the depth of maximum shear stress in addition to a 350 percent increase at a depth of 13.0 μm (0.5 mil).

Appendix – Derivation of Residual Stress Effect on Maximum Shear Stress

It is well known that classical rolling-element fatigue begins in the subsurface zone of maximum shear stress.[11-12] Therefore, to determine the effect of residual stress on rolling-element fatigue in gears, it is necessary to analyze the effect of residual stress on the maximum shear stress below the surface. The maximum shear stress at any point in a stressed volume below a rolling line-contact load is

$$(\tau_{\max})_y = \frac{1}{2} (S_z - S_y) \tag{A1}$$

$$(\tau_{\max})_x = \frac{1}{2} (S_z - S_x) \tag{A2}$$

where S_z is the principal compressive stress in a direction normal to the contact area, S_y is the principal comprehensive parallel stress to the direction of rolling,[13] and S_x is the principal stress normal.

For rollers or gear teeth loaded statically, the maximum theoretical shear stress occurs in the y-z plane since the stress in the y, or rolling, direction is less than the stress in the x

direction. Therefore, the maximum shear stress is

$$\tau_{max} = \frac{1}{2}(S_z - S_y) \tag{A3}$$

If the residual stresses are equal in the x and y directions, for the line contact in the y-z plane the maximum shear stress including the residual stress is

$$(\tau_{max})_r = \frac{1}{2}[S_z - (S_y + S_{ry})] \tag{A4}$$

$$(\tau_{max})_r = t_{max} - \frac{1}{2}S_{ry}$$

where S_{ry} is the residual stress in the y direction and is positive for tensile stress and negative for compressive stress. From Reference 13 for line contact of rollers

$$\tau_{max} = -0.30025\frac{b}{\Lambda} \tag{A5}$$

where b is the half width of the Hertzian contact,

$$b = \frac{2P_N}{\pi L S_{max}} \tag{A6}$$

and Λ for a contact of two rollers of the same material is

$$\Lambda = 4\frac{R_1R_2}{R_1+R_2}\left(\frac{1-\delta^2}{E}\right) \tag{A7}$$

If the rollers are of the same radius,

$$\Lambda = 2R\left(\frac{1-\delta^2}{E}\right) \tag{A8}$$

Where

- P_N normal load, N (lb)
- S_{max} maximum Hertz stress, N/m^2 (psi)
- R_1R_2 radius of curvature of the two rollers, m (in.)
- δ Poisson's ratio
- E Young's Modulus, N/m^2 (psi)

Substituting equations (A6) and (A8) into equation (A5) for τ_{max} results in

$$\tau_{max} = -0.30025\frac{P_N}{\pi L S_{max}}\left[\frac{E}{R(1-\delta^2)}\right] \tag{A9}$$

If equation (A9) is substituted into equation (A4),

$$(\tau_{max})_r = -0.30025\frac{P_N}{\pi L S_{max}}\left[\frac{E}{R(1-\delta^2)}\right] - \frac{1}{2}S_{ry} \tag{A10}$$

For steel gears $E = 207\times10^9$ N/m^2 (30×10^6 psi) and $\delta = 0.30$; therefore, equation (A10) becomes for SI units

$$(\tau_{max})_r = -21.74\times10^9\frac{P_N}{LS_{max}R} - \frac{1}{2}S_{ry} \tag{A11a}$$

and for U.S. customary units

$$(\tau_{max})_r = -3.15\times10^6\frac{P_N}{LS_{max}R} - \frac{1}{2}S_{ry} \tag{A11b}$$

where S_{ry} can be either compressive or tensile. When gears are shot peened, the residual stress is compressive and, therefore, reduces the maximum shear stress.

Since the rolling-element fatigue life of gears is inversely proportional to the maximum shear stress to the ninth power,[14]

$$\left.\begin{array}{l} L \sim \left(\dfrac{1}{\tau_{max}}\right)^9 \\ \text{or} \\ L \sim \left[\dfrac{1}{(\tau_{max})_r}\right]^9 \end{array}\right\} \tag{A12}$$

From equation (A4), where $(\tau_{max})_r = \tau_{max} - 1/2\,(S_{ry})$,

$$L \sim \left[\frac{1}{\tau_{max} - 1/2\,(S_{ry})}\right]^9 \tag{A13}$$

using a life ratio of L_1 and L_2

$$\frac{L_1}{L_2} = \left[\frac{\tau_{max} - 1/2\,(S_{ry})_2}{\tau_{max} - 1/2\,(S_{ry})_1}\right]^9 \tag{A14}$$

When the residual stress developed by the shot peening of the gear teeth is known, the change in life produced by shot peening can be determined from equation (A14).

References

1. MOORE, H. F.: "Shot Peening and the Fatigue of Metals." American Foundry Equipment Co., 1944.
2. STRAUB, J. C.: "Shot Peening in Gear Design." AGMA Paper 109.13, June 1964.
3. VALENTINE, K. B.: "Recrystallization as a Measurement of Relative Shot Peening Intensities." Am. Soc. Met. Trans. Q., Vol. 40, 1948, pp. 420–434.
4. ZARETSKY, ERWIN V.: et al.: "Effects of Component Differential Hardness on Residual Stress and Rolling-Contact Fatigue." NASA TN D-2664, 1965.
5. ZARETSKY, E. V.; PARKER, R. J.; and ANDERSON, W. J.: "Component Hardness Differences and Their Effect on Bearing Fatigue." J. Lub. Technol., Vol. 89, No. 1, Jan. 1967, pp. 47-62.
6. DOWSON, D.; and HIGGINSON, G. R.: "Elasto-Hydrodynamic Lubrication." Pergamon Press, 1966, p. 96.
7. JOHNSON, LEONARD G.: "The Statistical Treatment of Fatigue Experiments." Elsevier Pub. Co., 1964.
8. CHRISTENSON, A. L., ed.: "Measurement of Stress by X-Ray." SAE HS-182, Aug. 1971.
9. PREVEY, PAUL S.: "Method of Determining the Elastic Properties of Alloys in Selected Crystallographic Directions for X-Ray Defraction Residual Stress Measurements." Adv. X-Ray Anal., Vol. 20, 1977, pp. 345-354.

(continued on page 48)

TECHNICAL CALENDAR

January 28-30 — Fundamentals of Industrial & Manufacturing Engineering

The Society of Manufacturing Engineers is sponsoring an educational program on the "Fundamentals of Industrial and Manufacturing Engineering," to be held January 28-30, 1986 at the Sheraton-Sand Key Resort in Clearwater Beach, Florida. This clinic is an overview of the basic elements of running a manufacturing engineering operation in today's changing industry. Methods engineering, production standards, wage incentives, production planning and profit/cost control are some of the areas that will be covered.

March 3-5 — 2nd World Conference of Gearing
Institute de l'Engrenage et des Transmissions
Paris, France

The Paris Congress has brought together various groups of technicians, practitioners, buyers, production, lubrication and control experts (150 speakers from all over the world) to present the results of their research on gearing techniques. To obtain further information contact: Maurice Allard, Director, Institute de l'Engrenage et des Transmission, 162 Boulevard Malesherbes, 75017, Paris, France. Telephone: 43.80.04.09

March 17-19 — International Conference on Austempered Ductile Iron, Ann Arbor, Michigan

For further information contact: Dale Breen, Gear Research Institute, P.O. Box 353, Naperville, IL 60566, Telephone: (312) 355-4200.

AGMA ISSUES CALL FOR PAPERS

In preparation for the 1986 Fall Technical Meeting of the American Gear Manufacturers Association, AGMA President Walter Rye has issued a "call for papers."

Each year, the AGMA conducts what has become the foremost meeting in the U.S. for discussion of gear design and manufacturing technical points. The 1985 meeting, held at the Fairmont Hotel in San Francisco October 14-16, saw sixteen major papers presented by representatives of the foremost gear design people from around the world. The 1986 meeting, to be held at the Hyatt Regency in Chicago, October 5-8 will offer a similar opportunity for the leaders in this industry.

Individuals who wish to be considered for presentation should submit an abstract of the paper to Leonard Haas, Vice President, Technical Division, c/o AGMA Headquarters, 1500 King Street, Suite 201, Alexandria, VA 22314. Abstracts must be received no later than February 1, 1986. For more details, contact Bill Daniels of the AGMA staff at (703) 684-0211.

ERRATA:

Correction: we wish to apologize to Yefim Kotlyar for inadvertently omitting his biography on the article Hob Length Effects, September/October 1985.

Author:

MR. YEFIM KOTLYAR *is presently an Application Engineer with American Pfauter Limited. He received a M.S. in Mechanical Engineering from Odessa Marine Institute in Odessa, U.S.S.R. in 1972. After graduation, he was employed as a Mechanical Engineer at Tashkent Agricultural Machinery Institute from 1973 to 1979. Current research interests include developing mathematics for computer programs for various gear cutting applications.*

The Editors wish to make the following correction to Hob Length Effects, September-October 1985:

Formula page 18, col. 2 should read:

$$B = X = \frac{-b + \sqrt{b^2 - 4 \times a \times c}}{2 \times a}$$

Formula page 48, top, should read:

For first approximation Y can be set equal to PD/2 so $Y_1 = PD/2$

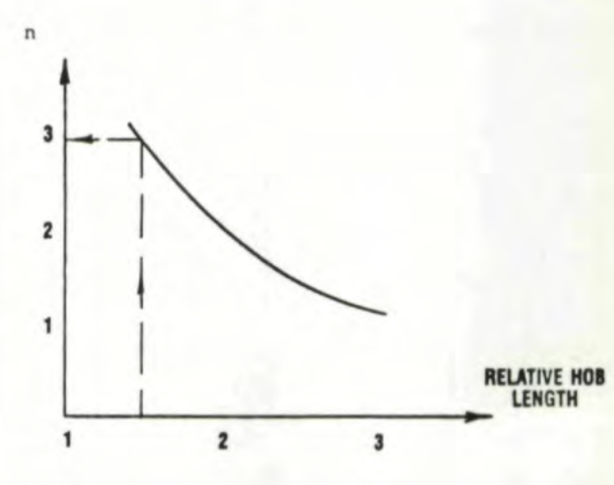

Fig. 4

Are you missing out? If there are back issues that you would like to receive, there are limited back issues available at a cost of $7.00 per issues in the USA, $15.00 per issue outside of the USA. Below is listed a complete index for all issues. (Foreign payments must be in US funds, drawn on a U.S. Bank) Checks must accompany requests.

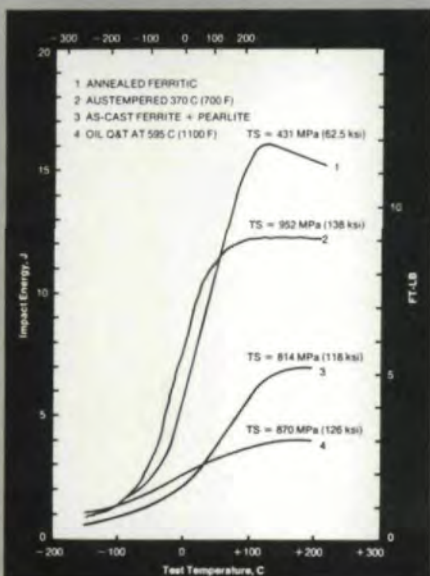

Fig. 1 – Impact properties of indicated nodular irons. AUSTEMPERED NODULAR CAST IRONS, Jay Janowak, Amax, & Robert Barr, Vol. 2, No. 2.

Fig. 2 – Analytical inspection charts showing the effects of runout. GEAR INSPECTION AND CHART INTERRUPTATION, Robert Moderow, Illinois Tool Works, Vol. 2, No. 3.

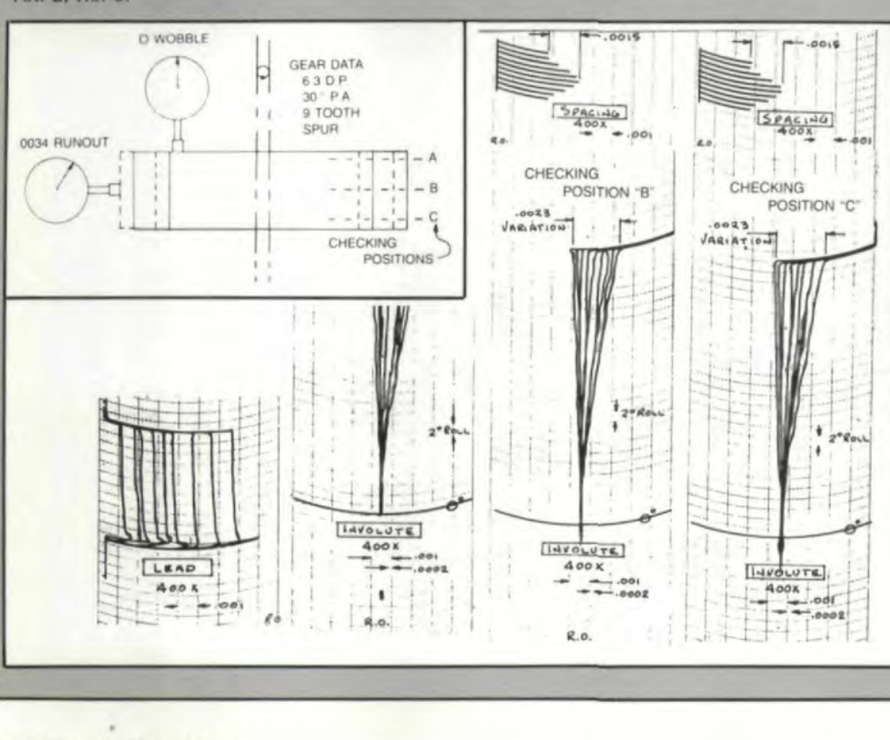

Fig. 3 – SINGLE FLANK TESTING OF GEARS by Robert Smith, Gleason Works, Vol. 1, No. 1.

Vol. 2, No. 3

Fig. 4 – Effect of grain shape on the rate of wear flat development, TECHNOLOGICAL FUNDAMENTALS OF CBN BEVEL GEAR FINISH GRINDING, Vol. 2, No. 6

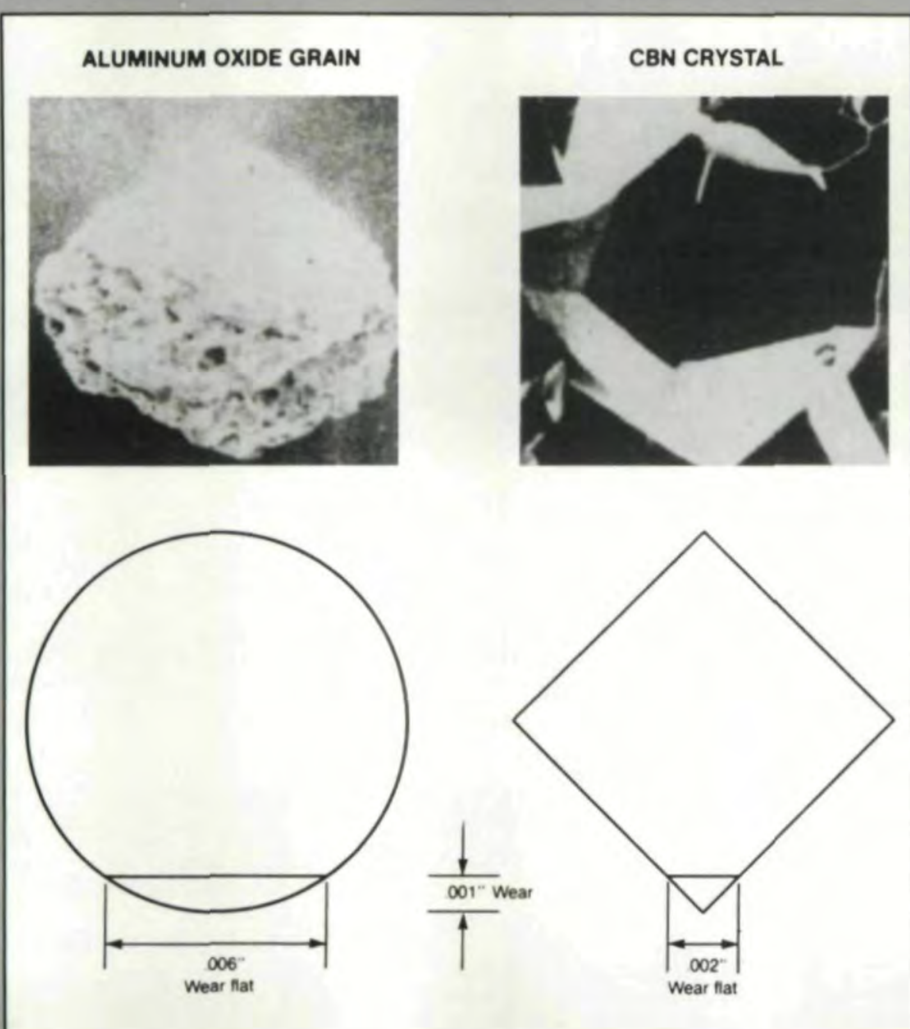

Vol. 2, No. 4

Vol. 2, No. 5

Vol. 2, No. 6

GEAR TECHNOLOGY
The Journal of Gear Manufacturing

1425 Lunt Ave.
P.O. Box 1426
Elk Grove Village, IL 60007

BACK TO BASICS...

The Process of Gear Shaving

by
John P. Dugas
National Broach & Machine
A Division of Lear Siegler, Inc.
Mt. Clemens, Michigan

Gear shaving is a free-cutting gear finishing operation which removes small amounts of metal from the working surfaces of the gear teeth. Its purpose is to correct errors in index, helical angle, tooth profile and eccentricity. The process can also improve tooth surface finish and eliminate, by crowned tooth forms, the danger of tooth end load concentrations in service. Shaving provides for form modifications that reduce gear noise. These modifications can also increase the gear's load carrying capacity, its factor of safety and its service life.

Gear finishing (shaving) is not to be confused with gear cutting (roughing). They are essentially different. Any machine designed primarily for one cannot be expected to do both with equal effectiveness, or equal economy.

Gear shaving is the logical remedy for the inaccuracies inherent in gear cutting. It is equally effective as a control for these troublesome distortions caused by heat treatment.

The form of the shaving cutters can be re-ground to make crown and profile allowance for different heat treatment movements due to varying heats of steel. The gear shaving machine can also be reset to make allowance for lead change in heat treatment.

The gear shaving process can be performed at a high production rate. Machines are available to shave external spur or helical gears up to 180" in diameter. Other machines are also available for internal spur or helical gears.

For best results of shaving, the hardness of the gear should not exceed 30-32 Rc scale. When stock removal is kept to the recommended limits, and gears are properly qualified, the shaving process will finish gear teeth in the 7 to 10 pitch range to the following accuracies: involute profile .0002; tooth-to-tooth spacing .0003; lead or parallelism .0002. In any event, it should be remembered that gear shaving can remove 65 to 80% of the errors in the hobbed or shaped gear. *It will make a good gear better. The quality of the shaved gear is dependent to a large degree upon having good hobbed or shaped gear teeth.*

Basic Principles of Gear Shaving

The rotary gear shaving process uses a gashed rotary cutter, (Fig. 1), in the form of a helical gear having a helix angle different from that of the gear to be shaved.

When the cutter and work gear are thus rotated in close mesh, the edge of each gash, as it moves over the surface

---

AUTHOR:

MR. JOHN P. DUGAS *is the Chief Gear Tool Engineer at National Broach & Machine Div., Lear Siegler, Inc., Mt. Clemens, Michigan. His experience encompasses 20 years of design, analysis and development of gear finishing tools. He has attended Ohio State University and the University of Mass. He is an active member of several AGMA committees and annually participates in the SME Gear Manufacturing Symposium.*

of a work gear tooth, shaves a fine hair-like chip, somewhat like that produced by a diamond boring tool.

The finer the cut, the less the pressure required between tool and work, eliminating the tendency to cold-work the surface metal of the work gear teeth.

This process is utilized in a shaving machine, (Fig. 2), which has a motor-driven cutter head and a reciprocating work table. The cutter head is adjustable to obtain the desired crossed axes relationship with the work. The work, carried between live centers, is driven by the cutter.

During the shaving cycle, the work is reciprocated parallel to its axis across the face of the cutter and up-fed an increment into the cutter with each stroke of the table. This shaving cycle (axial) is one of several methods.

The Crossed Axes Principle

To visualize the crossed axes principle, consider two parallel cylinders of the same length and diameter (Fig. 3).

When brought together under pressure, their common contact surface is a rectangle having the length of a cylinder and width which varies with contact pressure and cylinder diameter.

When one of these cylinders is swung around, so that the angle between its axis and that of the other cylinder is increased up to 90 degress, their common contact plane remains

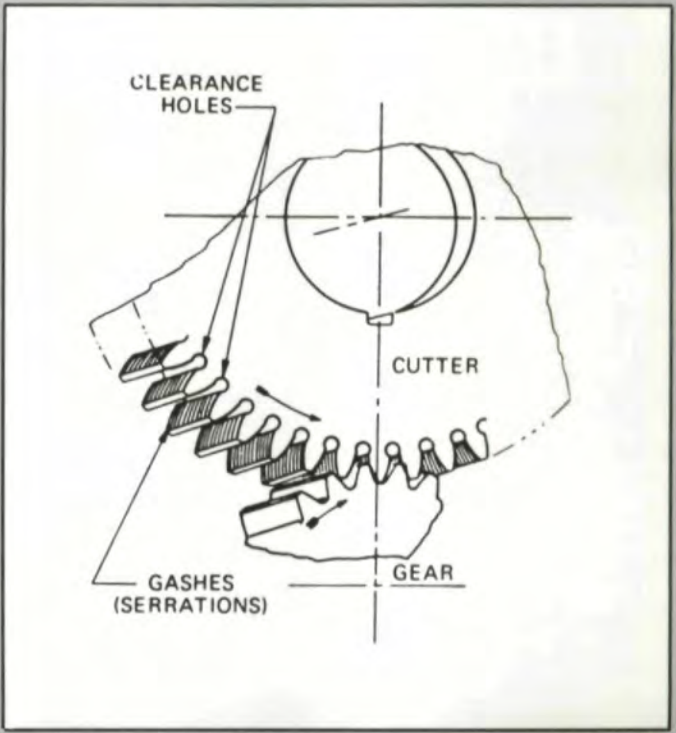

Fig. 1 – Work gear in crossed axes mesh with rotary shaving cutter mounted above.

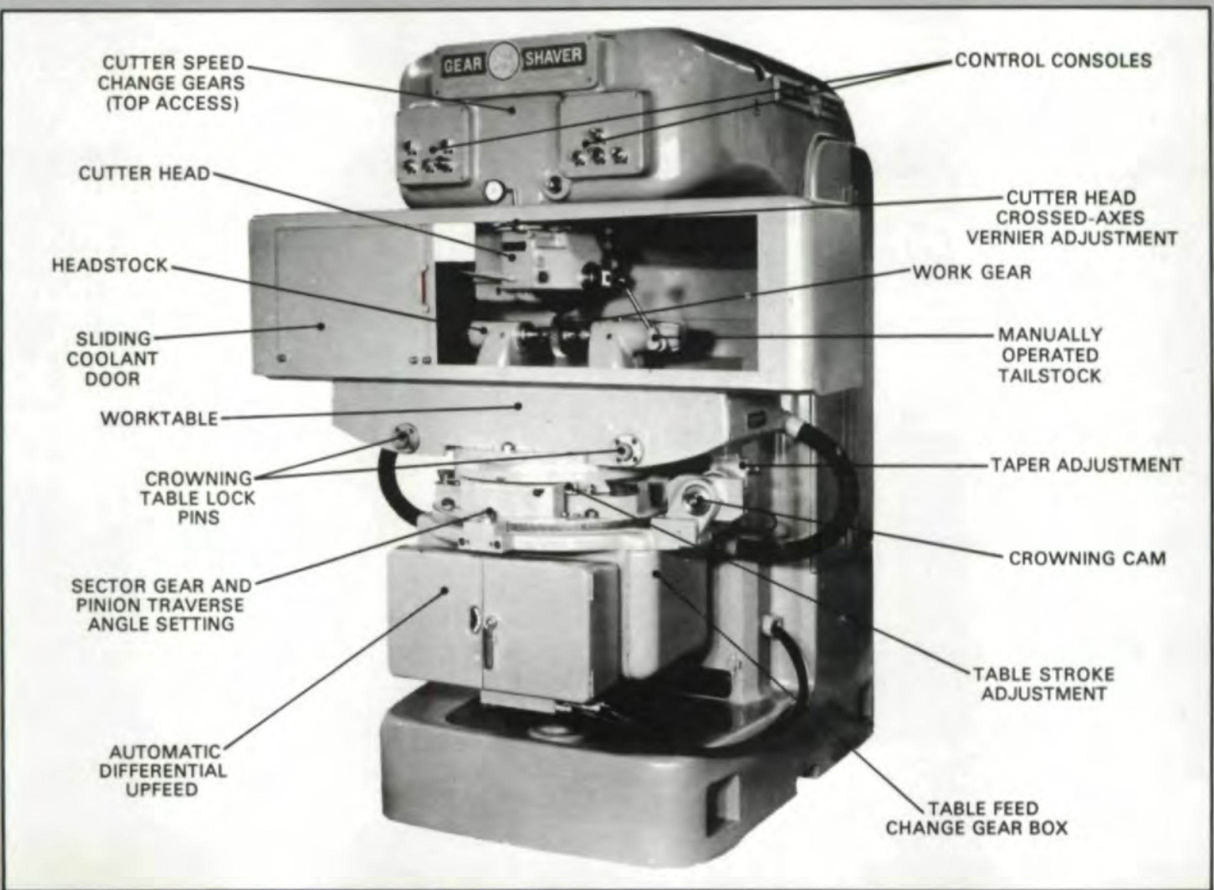

Fig. 2 – Operating components of a knee-and-column type shaving machine.

a parallelogram, but its area steadily decreases as the axial angle increases.

The same conditions prevail when, instead of the two plain cylinders, a shaving cutter and a work gear are meshed together. When the angle between their axes is from 10° to 15°, tooth surface contact is reduced and pressure required for cutting is small.

For shaving, the cutter and work gear axes are crossed at an angle usually in the range of 10° to 15° or approximately equal to the difference of their helical angles.

Crossing of the axes produces reasonable uniform diagonal sliding action from the tip of the teeth to the root. This not only compensates for the non-uniform action typical of gears in mesh on parallel axes, but also provides the necessary shearing action for metal removal.

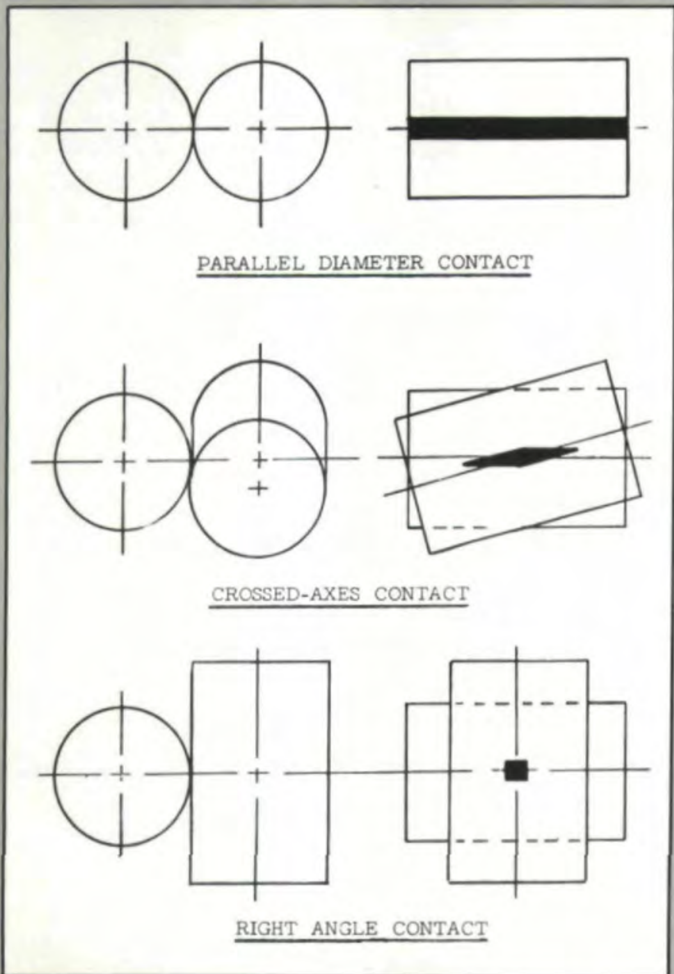

Fig. 3—How the contact between cylinders changes as the angle between their axes is varied.

Relation Between Cutting and Guiding Action

Increasing the angle between the cutter and work gear axes increases cutting action but, as this reduces the width of the contact zone, guiding action is sacrificed. Conversely, guiding action can be increased by reducing the angle of crossed axes, but at the expense of cutting action. At zero angle, there is no cutting.

The spur and helical gears at the left in (Fig. 4), were shaved without table reciprocation. They show the band of cutter contact less than gear face width; and also a deeper cut in the middle of the gear than on either side.

The gears in the center of (Fig. 4), were shaved with only about 1/4 in. table reciprocation. The profiles of these teeth are perfect over the distance of reciprocation, but they fade out at each end. The chordal thickness along this 1/4 in. length is less than that at the ends.

Fig. 4—The cut developed with varying amounts of cutter reciprocation in shaving spur gears, top, and helical gears, bottom.

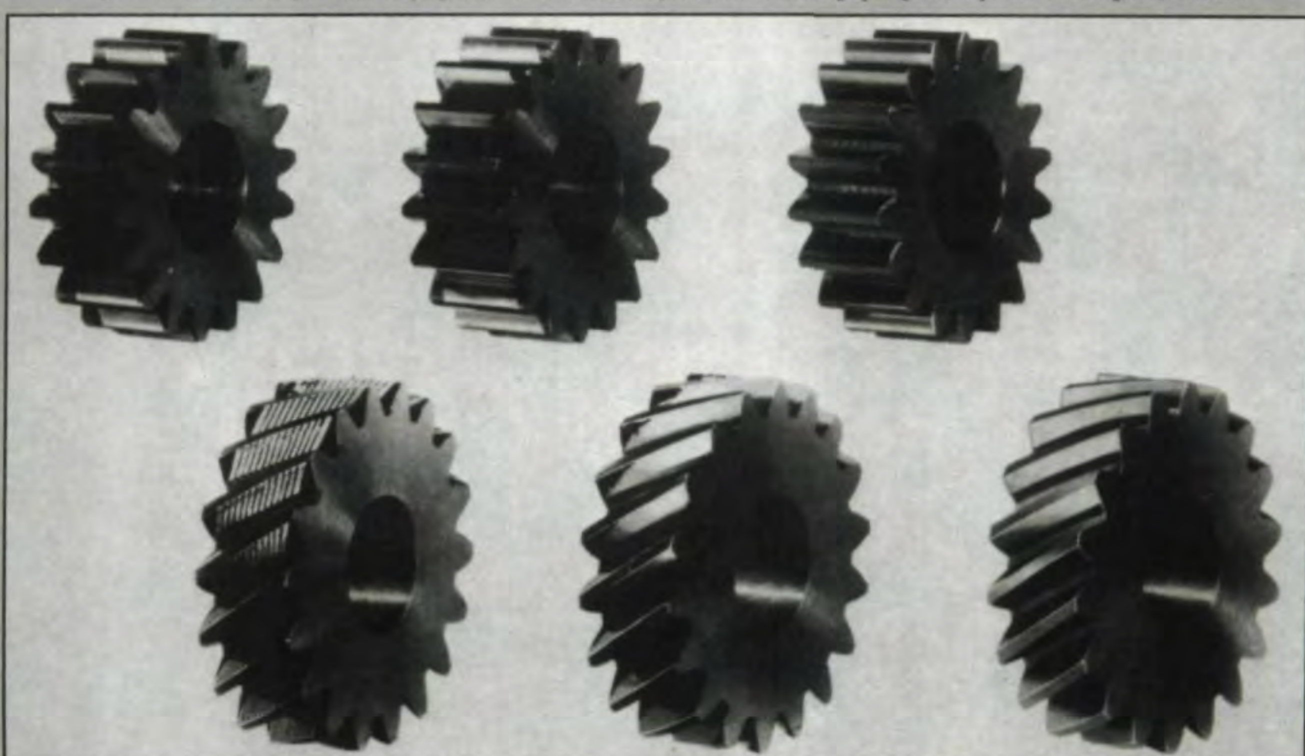

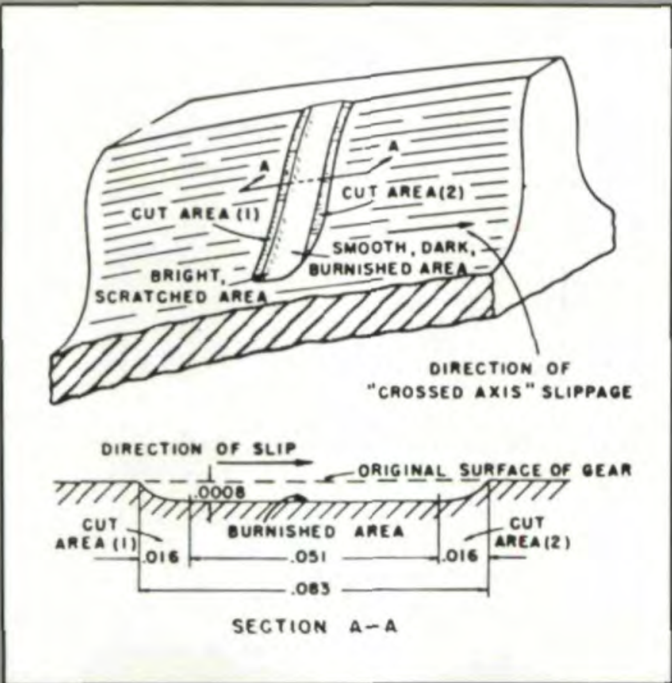

Fig. 5—Gear shaving is a combination of both cutting and burnishing.

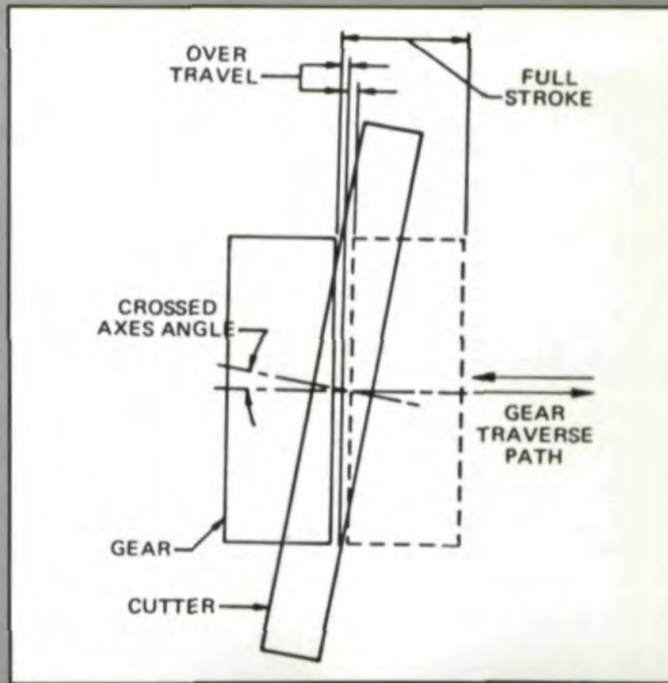

Fig. 6—Axial shaving (conventional)

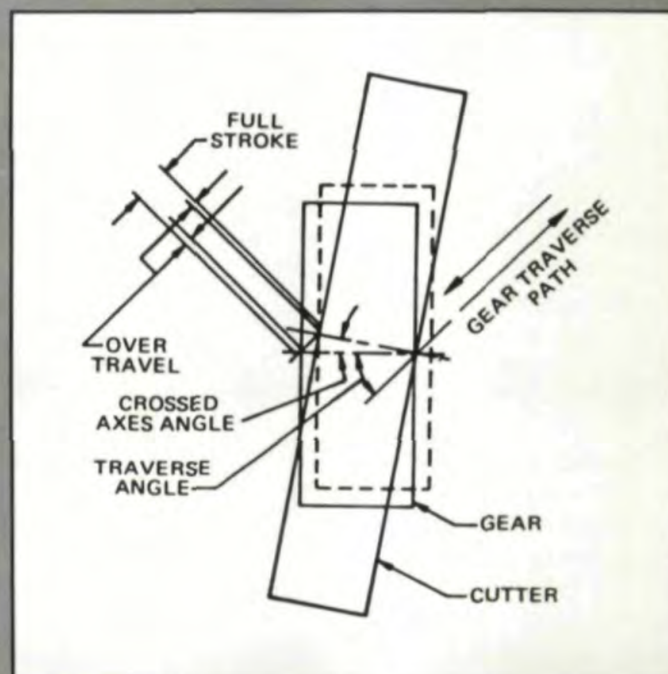

Fig. 7—Diagonal shaving

Gears at the right in (Fig. 4), were shaved with full reciprocation and, therefore, have been finished to the full depth over the entire face. Tooth thickness may be decreased by increasing the up-feed of work toward the cutter.

Shaving cutters are high precision, hardened and ground, high speed steel generating tools, held to Class A or AA tolerances in all principle elements. The gashes in the shaving cutter extend the full length of the profile, termination in the clearance space or oil hole at the bottom. These clearance spaces provide unrestricted channels for a constant flow of coolant to promptly dispose of chips. They also permit uniform depth of serration penetration and increased life of the cutter. The shaving cutter is rotated at high speeds, up to 400 and more surface feet per minute. Feed is fine and the tool contact zone is restricted. Cutter life depends on several factors; operating speed, feed, material and hardness of the work gear, its required tolerances, type of coolant, and size ratio of the cutter to work. Rotary shaving cutters are available in tooth size ranges from 120 diametral pitch to 1 diametral pitch, with outside diameters up to 16", and widths up to 4⅞ in.

Shaving Methods

There are four basic methods of gear shaving:

1) Axial or conventional method
2) Diagonal method
3) Tangential or underpass method
4) Plunge

Axial shaving (Fig. 6) is widely used in low and medium production operations. It is the most economical method for shaving wide face width gears. In this method, the traverse path is along the axis of the work gear. The centerline of crossed axes is passed through the entire face of the gear. The number of strokes may vary due to the amount of stock to be removed. In axial shaving, in order to crown the work gear teeth, it is necessary to rock the machine table by use of the built-in crowning mechanism.

Diagonal shaving (Fig. 7) is used primarily in medium and high production operations. By use of this method, shaving times are reduced by as much as 50%. In diagonal shaving, the sum of the traverse angle and the crossed axes angle is limited to approximately 55° unless special differential type serrations are used; otherwise, the serrations will track. Relative face width of the gear and the shaving cutter has an important relationship with the diagonal traverse angle. A wide face work gear and a narrow shaving cutter restrict

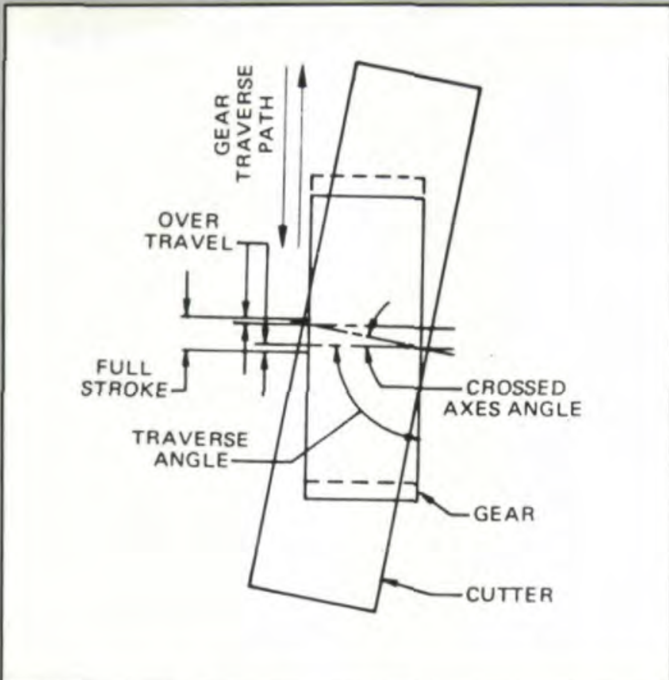

Fig. 8 – Tangential shaving (underpass)

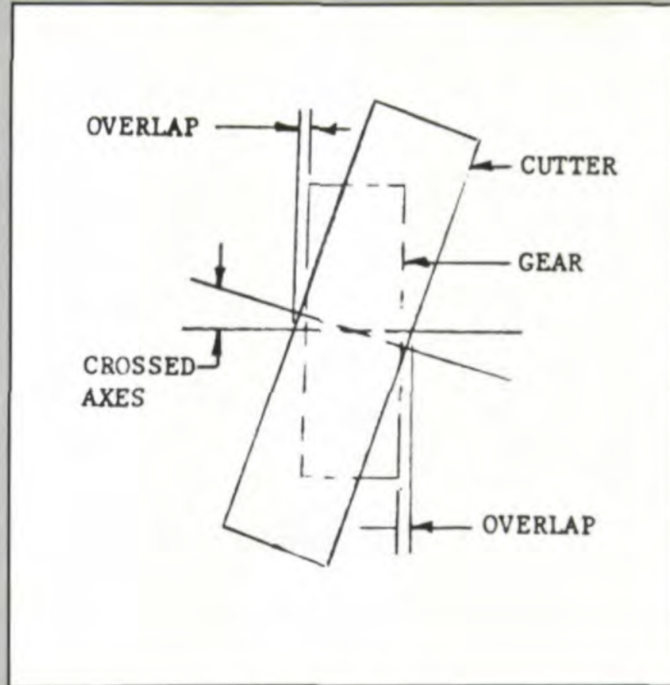

Fig. 9 – Plunge shaving

the diagonal traverse to a small angle. Increasing the cutter face width permits an increase in the diagonal angle. Crowning the gear teeth can be accomplished by rocking the machine table providing the sum of the traverse angle and crossed axes angle does not exceed 55°. When using high diagonal angles, it is preferable to grind a reverse crown (hollow) in the lead of the cutter.

In tangential (underpass) shaving (Fig. 8), the traverse path of the work is perpendicular to its axis. Tangential shaving is used primarily in high production operations and is ideally suited for shaving gears with restricting shoulders. This method of shaving has restriction. First, the serration on the cutter must be of a special differential type. Second, the face width of the cutter must be larger than that of the work gear.

Diagonal shaving has some built-in advantages over axial shaving. In most cases, it is much faster than axial. In many cases, up to 50% faster. With diagonal traverse, the cutting is not restricted to a small zone of the cutter as it is in axial shaving, but is migrated across the cutter face. Consequently, cutter life is extended.

Plunge shaving (Fig. 9) is used in high production operations. In this method, the work gear is fed into the shaving cutter with no table traverse. The shaving cutter must have special differential type serrations or tracking will occur. To obtain a crowned lead on the work, it is necessary to grind into the shaving cutter lead a reverse crown or hollow. In all cases of plunge shaving, the face width of the tool must be greater than that of the work. The advantage of plunge shaving is very short cycle times. The disadvantage is lower tool life due to the speed stock being removed.

Mounting the Work Gear

The work gear should be shaved from the same locating points or surfaces used in the preshaving operation. Locating faces should be clean, parallel and square with the gear hole. Gears with splined holes may be located from the major diameter, side of the splined teeth or minor diameter. When shaved from the centers, the true center angle should be qualified and surfaces should be free of nicks, scale and burrs.

Locating points on the work arbors and fixtures should be held within a tolerance of 0.0002 in. The arbor should fit the gear hone snugly. Head and tailstock centers should run within 0.0002 in.

For the most dependable results, gears should be shaved from their own centers whenever possible. If this is not possible, rigid, hardened and ground arbors (Fig. 10), having large safety centers would be used. Locating faces should be the same as those used in hobbing or shaper cutting.

Integral tooling is another method which is becoming popular, especially in high production shops. This consists of hardened and ground plugs instead of centers, on the head and tailstocks. These plugs are easily detached and replaced when necessary. They locate in the bore and against the faces of the work gear.

Coolants

It is very important to use the proper cutting oil or coolant for gear shaving, the basic essential of which will be found in the following:

For steels, use a sulphur base oil having a sulphur content of 3 to 3.5%.

For bronze, cast iron and aluminum use a mixture of eight parts of kerosene and one part of light machine oil. Some types of quenching and honing oils are also satisfactory.

For plastics, use a water-soluble oil mixture of approx-

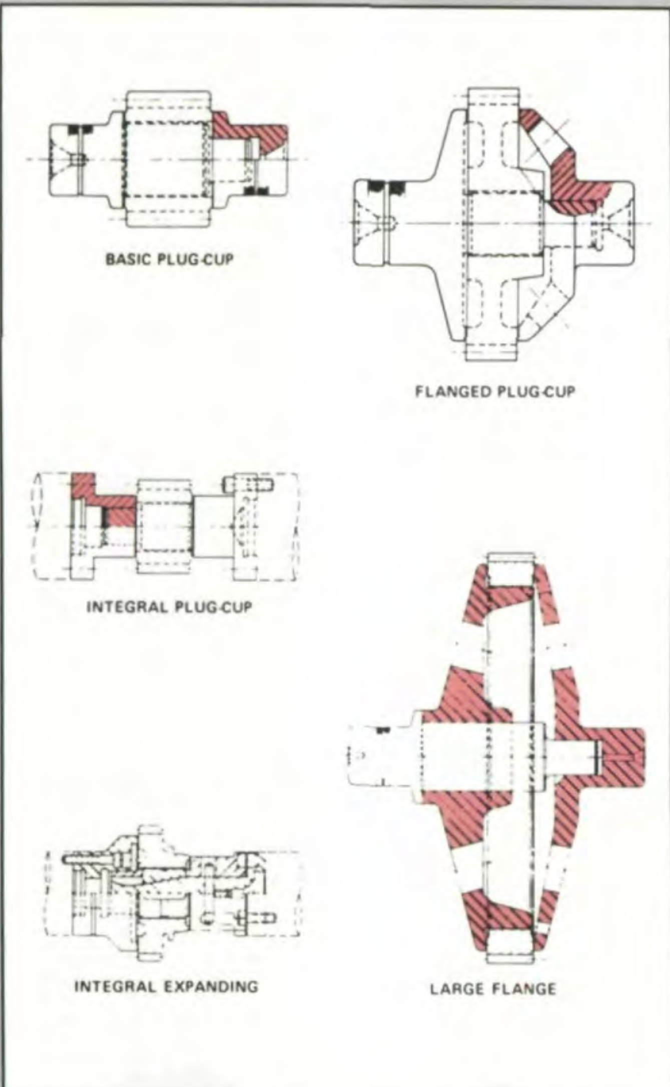

Fig. 10 – Typical gear shaving arbors for external gears.

imately one part oil and twenty parts water.

The type of coolant and the degree of its contamination directly affect cutter service life and the finish of the shaving tooth surfaces. Avoid the use of a cutting oil that is too thin as this will cause chip scratch on the gear teeth faces. Chip baskets should be cleaned periodically if a supplementary filter is not used.

The cutting oil should have a viscosity of about 135 S.S.U. at 100°F. A magnetic chip separator in the coolant circuit will help reduce contamination.

Feeds and Speeds

The following are formulas for determining shaving cutter and work gear speeds (rpm):

$$\text{Cutter Rpm} = \frac{\text{Desired surface Ft. Per Minute}}{\dfrac{\text{Cutter Diameter (In.)} \times \pi}{12}}$$

$$\text{Gear Rpm} = \text{Cutter Rpm} \times \frac{\text{No. of Teeth in Cutter}}{\text{No. of Teeth in Gear}}$$

For conventional shaving, about 0.010 in. per revolution of gear is considered a good starting point and becomes a factor in the following formula:

$$\text{Table Feed (ipm)} = 0.010 \times \text{Gear Rpm}$$

For diagonal shaving, an "Effective Feed Rate" of approximately 0.040 in. per revolution of gear is considered a good starting point. Effective feed rate is the speed at which the point of crossed axes migrates across the face of the gear and cutter. The following is the formula for determining the table travese rate (ipm) to produce 0.040 in. effective feed rate:

$$R_f = \frac{\text{Sine Traverse Angle}}{\text{Tangent Crossed Axes Angle}} + \text{Cosine Traverse Angle}$$

$$\text{Table Traverse Rate (ipm)} = \frac{0.040 \times \text{Gear Rpm}}{R_f}$$

The maximum theoretical diagonal traverse angle is determined by:

$$\text{Tangent Max. Traverse Angle} = \frac{\text{Cutter Face Width} \times \text{Sine Crossed Axes Angle}}{\text{Gear Face} - (\text{Cutter Face X Cosine Crossed Axes Angle})}$$

Supplementary 1

Approximate Stroke for Tangential and Diagonal Shaving for Machine with Upfeed

$$\frac{\sqrt{\left[\dfrac{.0005}{\operatorname{Tan} \emptyset_n} + C\right]^2 - C^2}}{\operatorname{Sin} \partial} + \frac{.5\, F \operatorname{Sin} \times}{\operatorname{Sin} (\times + \partial)} = \text{FRONT STROKE}$$

Rear Stroke Same As Front Stroke

For Machine Without Upfeed

$$\frac{\sqrt{\left[\dfrac{.0005 + .5\, S}{\operatorname{Tan} \emptyset_n} + C\right]^2 - C^2}}{\operatorname{Sin} \partial} + \frac{.5\, F \operatorname{Sin} \times}{\operatorname{Sin} (\times + \partial)} = \text{FRONT STROKE}$$

Rear Stroke Same As Above (with upfeed)

$$C = \frac{\text{(Approx.) Pitch Dia. Cutter + Pitch Dia. Gear}}{2}$$

∂ = Diagonal Traverse Angle
X = Cross Axis Angle
$\emptyset_n$ = Normal Pressure Angle
F = Gear Face Width
S = Shaving Stock on Gear Tooth Thickness (Approx.)

Supplementary 2

(continued on next page)

4 DP 20° PA 150 TEETH 30° HELIX OR SPUR

MATERIAL: 8620 180-220 BHN.

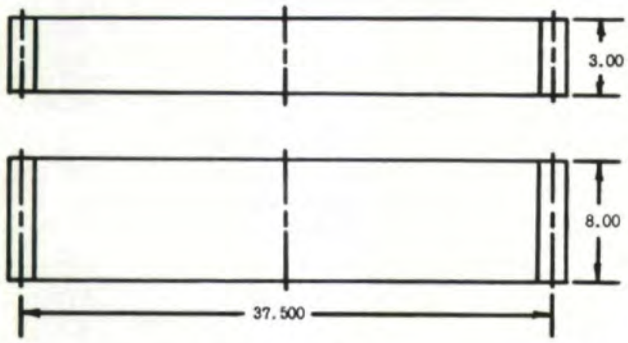

AXIAL SHAVING

3" FACE	41.7 Min.
8" FACE	108.5 Min.

SHAVING CUTTER - 12" DIA x 1" FACE

Supplementary 3

10 DP 20° PA 60 TEETH SPUR

MATERIAL: 8620 180-220 BHN.

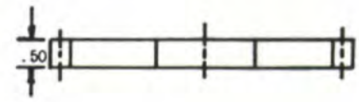

.500 FACE WIDTH GEAR

METHOD	MIN.	C. FACE
AXIAL	1.10	1.000
DIAGONAL	1.05	1.000
TANGENTIAL	.84	1.000
PLUNGE	.50	1.000

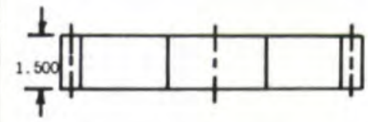

1.500 FACE WIDTH GEAR

METHOD	MIN:	C: FACE
AXIAL	2.87	1.000
DIAGONAL	1.47	1.250
TANGENTIAL	1.05	1.750
PLUNGE	.75	1.750

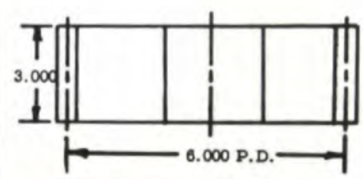

3.000 FACE WIDTH GEAR

METHOD	MIN.	C. FACE
AXIAL	5.52	1.000
DIAGONAL	2.10	2.750
TANGENTIAL	1.68	3.250
PLUNGE	1.50	3.250

Supplementary 4

19 DP 20° PA 21 TEETH SPUR and 20° HELIX

MATERIAL: 8620 180-220 BHN.

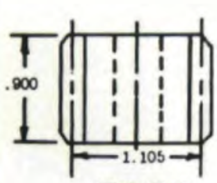

SPUR GEAR

METHOD	TIME	C: FACE
AXIAL	47 SEC.	.750
DIAGONAL	18 SEC.	1.000
TANGENTIAL	14 SEC.	1.150
PLUNGE	10 SEC.	1.150

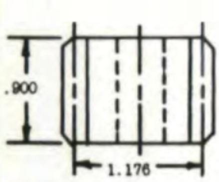

20° HELICAL GEAR

METHOD	TIME	C. FACE
AXIAL	47 SEC.	.750
DIAGONAL	18 SEC.	1.000
TANGENTIAL	14SEC.	1.150
PLUNGE	10 SEC.	1.150

Supplementary 5

16 DP 20° PA 70 TEETH SPUR and 20° HELIX

MATERIAL: 8620 180-220 BHN.

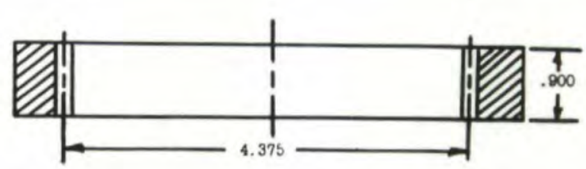

AXIAL SHAVING

SPUR	1.37 Min.
20° HELIX	1.37 Min.

SHAVING CUTTER - 3" DIA. x .750 FACE

Supplementary 6

(continued on page 48)

CLASSIFIED

Rates: Classified Display—$100 per inch (minimum 3") Type will be set to advertiser's layout or *Gear Technology* will set type at no extra charge. **Word Count:** 35 characters per line, 7 lines per inch.

Payment: Full payment must accompany classified ads. Mail copy to *Gear Technology*, P.O. Box 1426, Elk Grove Village, IL 60007. **Agency Commission:** No agency commission on classifieds.

Closing date: Ads must be received by the 25th of the month, two months prior to publication. **Acceptance:** Publisher reserves the right to accept or reject classified advertisements at his discretion.

HELP WANTED

DIRECTOR ENGINEERING

NEW YORK BASED, SMALL GROWING AEROSPACE CO.; EQUITY INCENTIVE; MILITARY, GEARING, ACTUATOR EXPERIENCE HELPFUL.

CALL (718) 932-8500
FRANK SUOZZI

Superior Electro Mechanical Component Service, Inc.
36-07 20th Ave.
Long Island City, NY 11105

HOBBER REBUILDING SPECIALISTS

Having trouble meeting today's demand quality control tolerances?

Let our factory trained and experienced staff return your machine to optimum operating condition.

We specialize in repairing, rebuilding and modernizing all makes of hobbers.

- Cleveland Rigidhobbers
- Gould & Eberhardt
- Barber Colman

PRESSMATION INC.
522 Cottage Grove Road
Bloomfield, Conn. 06002
(203) 242-8525

SUBCONTRACT WORK

SPIRAL BEVEL GEARS

Coniflex bevels to 34" diameter
Prototype or production up to 60" diameter
Breakdown work — fast turnaround
Complete machining, heat treat, lapping and testing
CALL US!

B&R MACHINING
PO Box 536
Sharon, TN 38255
1-800-238-0651

CIRCLE A-17 ON READER REPLY CARD

FOR SALE

PEREZ MACHINE TOOL

11 Ginger Court, East Amherst, New York 14051 • (716) 688-6982

Exclusive U.S.A. distributor for the Okamoto SHG-360, 400, 600 Gear Grinders

Designed to meet the requirements for *precision economical grinding of spur* and helical gears, . . .

For aircraft, automotive and machinery applications.

CIRCLE A-25 ON READER REPLY CARD

TELL OUR ADVERTISER'S . . .

YOU SAW IT IN GEAR TECHNOLOGY

There's still time . . . closing date for a classified ad in the March/April is **January 25th.**

GEAR TOOTH GRINDING & HONING ONLY

Production Quantities
3/4" P.D. to 27.5" P.D.;
3.5 D.P. and 11" Face

We have no turning, hobbing or shaping capability

ALLEGHENY GEAR CORP.
23 Dick Road
Depew, NY 14043
716-684-3811

CIRCLE A-18 ON READER REPLY CARD

THE PROCESS OF GEAR SHAVING . . .
(continued from page 46)

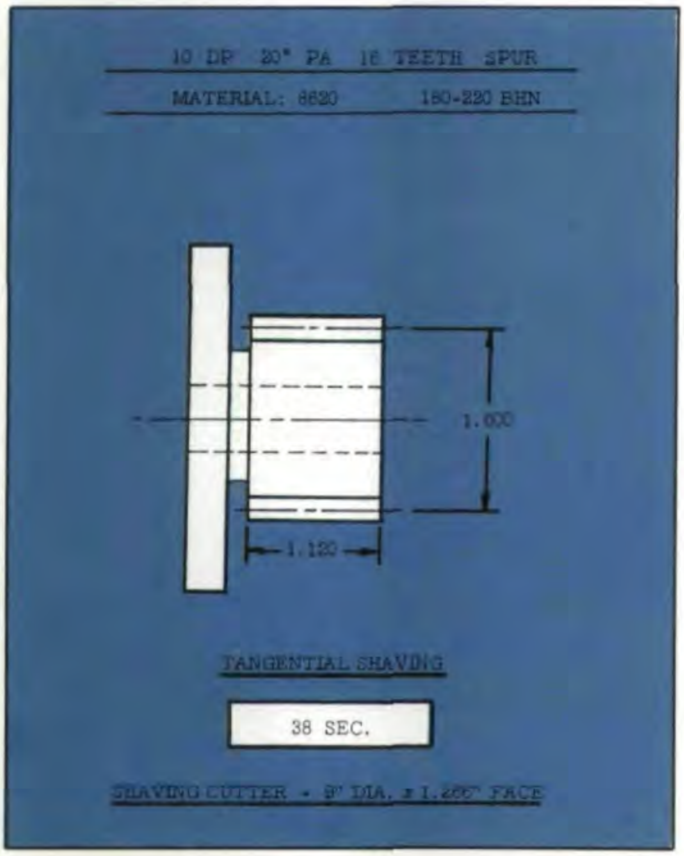

Supplementary 7

E-5 ON READER REPLY CARD

LOWER GRINDING COST . . .
(continued from page 21)

the trueing costs (not included here) these constitute the production costs per flute. This shows that corundum grinding is about 30% more expensive than CBN grinding. The superioity of CBN is likely to increase still further, assuming a rise in the labor and machine costs which determine production costs. Moreover, further developments may be expected in the relatively young CBN technology, on the basis of ongoing progress in fundamental knowledge.

Fig. 17 – CBN grinds more economically than corundum and gives better quality

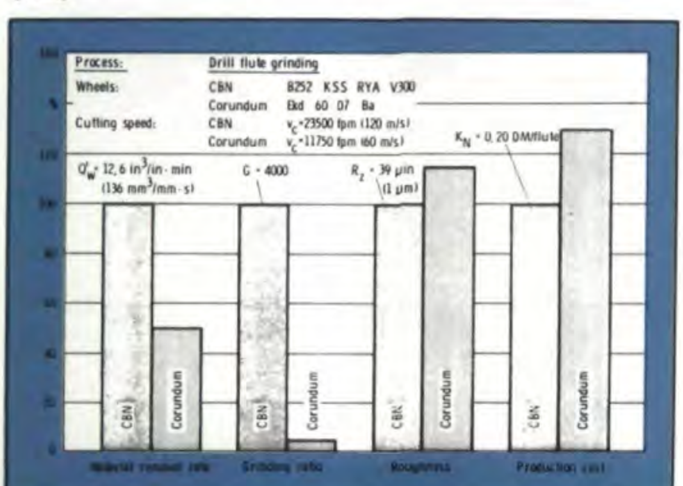

Summary

One of the main problems in the application of CBN wheels is the correct economical and technological design of the dressing process, i.e. trueing and sharpening. This paper presents methods for optimizing the dressing process, and in particular, the sharpening process. A process model for sharpening with a corundum sharpening stick is presented. The chip space of the grinding wheel is described as a function of wheel specification, setting parameters and duration of the sharpening process. The model for description of sharpening results can be used directly in practical application, since it includes only variables that can be regarded as known when the process design is made.

The technological advantages offered by the use of CBN must be offset against the main disadvantage of high grinding wheel cost. As the tool costs per workpiece are mainly influenced by wheel wear, the result of the present investigations show possibilities of improving wear behavior by adaptation of the grinding wheel specification. Possible measures might be the selection of suitable grit size, the use of a harder bond and an increase in grit concentration. An increase in grit concentration makes the grinding wheel more expensive, but in return it gives a clear improvement in the length of service life.

The machine concepts were also discussed as the prerequisite for economic application of this process. The following must be particularly stressed: high rigidity of the machine, high cutting speeds and drive powers and automated trueing and sharpening systems.

If the process is properly designed, it is at present possible to reduce the production costs per drill flute by approximately 30% as compared with corundum grinding.

E-1 ON READER REPLY CARD

EFFECT OF SHOT PEENING . . .
(continued from page 36)

10. TOWNSEND, D. P.; COY, J. J.; and ZARETSKY, E. V.: "Experimental and Analytical Load Life Relation for AISI 9310 Steel Spur Gears." Journal of Mechanical Design, Trans. ASME, Vol. 100, No. 1, Jan. 1978, pp. 54-60.
11. JONES, A. B.: "Metallographic Observations of Ball Bearing Fatigue Phenomena." Symposium on Testing of Bearings, ASTM, 1947, pp. 35-48; discussion, pp. 49-52.
12. CARTER, T. L.: et al: "Investigation of Factors Governing Fatigue Life with the Rolling-Contact Fatigue Spin Rig." Am. Soc. Lubr. Eng. Trans., Vol. 1, No. 1, Apr. 1958, pp. 23-32.
13. JONES, A. B.: "New Departure – Analysis of Stress and Deflections." Vol. I, New Departure, Div. Gen. Motors Corp., 1946, pp. 22.
14. LUNDBERG, G.; and PALMGREN, A.: "Dynamic Capacity of Rolling Bearings." Acta. Polytech. Scand., Mech. Eng. Ser., Vol. 1, No. 3, 1947.

E-4 ON READER REPLY CARD

CAN YOU GET CONSISTENT OVERPIN DIAMETER OF 0.0012" FROM COLD START?

You can, with Mitsubishi's new GA-Series Gear Hobbers!

Here's the reason why you can get such a consistent accuracy over hours of continuous running. To maintain the thermal stability of the machine, the hydraulic oil is maintained to a constant temperature by a refrigerating unit and the unit is isolated from the machine. The 36" wide 3-runway bed and heavy duty ball screws also plays a big role in maintaining high accuracy.

Not only is the machine accurate but also can withstand heavy duty cuts due to the robust construction of the machine and an AC servo motor driven direct hob drive mechanism. A hydraulically controlled backlash eliminator on the indexing table permits "reverse hand conventional cutting" which gives 4 to 5 times more cutter life on your tools.

Another prominent feature of the machine is the conversational "MENU" programming. Just key in the gear and hob data and select the type of material you are going to cut. The computer of the CNC will do the rest for you. No calculation of cutter path or selection of cutting parameters.

Needless to say, with a full CNC machine, the changeover time can be reduced to a maximum of 90%.

These are only a part of what our GA-series can do for you. For more information, write to our Bensenville office below or call, area code 312-860-4220 NOW!

SPECIFICATIONS

	GA250NC	GA40CNC
Maximum part diameter	10"	16"
Maximum DP	4	4
Maximum radial travel	8.26"	10"
Maximum axial travel	10.6"	10.6"
Worktable diameter	8.45"	16.5"
Hob speed range	200–600rpm	200–600rpm
Hob drive motor	10hp	10hp

MITSUBISHI
HEAVY INDUSTRIES, LTD.
5-1, Marunouchi 2-chome, Chiyoda-ku, Tokyo, Japan
Cable Address: HISHIJU TOKYO

Mitsubishi Heavy Industries America, Inc.
873 Supreme Drive, Bensenville, IL 60106 Phone: (312) 860-4220

CIRCLE A-9 ON READER REPLY CARD


ALLEN-BRADLEY